

Elucidating the mechanism of epidermal stem cell  
maintenance by cellular glycosylation and extracellular  
matrix protein

(糖鎖と細胞外マトリクスに着目した表皮幹細胞制御メカニズムの解明)

2020

筑波大学グローバル教育院

School of Integrative and Global Majors in University of Tsukuba

Ph.D. Program in Human Biology

Lalhaba Oinam



筑波大学  
University of Tsukuba

博士（人間生物学）学位論文  
Ph.D. dissertation in Human Biology



Elucidating the mechanism of epidermal stem cell  
maintenance by cellular glycosylation and extracellular  
matrix protein

(糖鎖と細胞外マトリクスに着目した表皮幹細胞制御メカニズムの解明)

2020

筑波大学グローバル教育院

School of Integrative and Global Majors in University of Tsukuba

Ph.D. Program in Human Biology

Lalhaba Oinam

## ACKNOWLEDGMENT

I would like to extend my sincere gratitude to my academic advisor Professor Hiromi Yanagisawa for her continuous guidance and support during my Ph.D. study and the project. I would also like to thank for her patience, motivation, and initiation for my collaborative project. Along with my academic advisor, I would like to thank my mentor Dr. Aiko Sada for her help in guiding the project, encouragement, insightful discussion, experimental planning, and her support in writing the paper, among other things.

Besides them, I would also like to thank Dr. Hiroaki Tateno, my collaborative mentor from AIST, Tsukuba, for his constant guidance and willingness to let me work in his laboratory and conduct experiments. I am also grateful to his technical staff for their help and advice during my research project.

I am also grateful to my dissertation committee members for their professional guidance, insightful comments, and hard questions.

I would also like to thank the laboratory members in the Hiromi Yanagisawa Laboratory. It has been a great pleasure to work along with them in my project and other projects.

Last but not least, I want to thank my parents and family members back home who have always been an inspiration and emotional support during the pursuit of this project and my Ph.D. I am indebted to Prof. Rakwal Randeep, and to my friend Mr. Manoj Kumar Yadav, Mr. Lokesh Kumar, and Mr. Yaqiu Wang, for their warm support and encouragement.

# CONTENTS

	<b>Page number</b>
<b>ACKNOWLEDGEMENT</b>	1
<b>CONTENTS</b>	2-4
<b>ABBREVIATIONS</b>	5
<b>List of Figures</b>	6
<b>Chapter 1: Distinct glycosylation patterns during epidermal stem cell aging</b>	7-27
1.1 Abstract	7
1.2 Introduction	8-9
1.3 Experimental Procedures	10-15
1.3.1 Mice	
1.3.2 Isolation of epidermal stem cells by flow cytometry	
1.3.3 Membrane protein isolation and quantification	
1.3.4 Lectin microarray	
1.3.5 Lectin blotting	
1.3.6 Detection of lectin binding to epidermal stem cells by flow cytometry	
1.3.7 RT <sup>2</sup> profiler for mouse glycosylation PCR array	
1.3.8 Mouse primary keratinocytes isolation and culture	
1.3.9 Lentivirus production and infection	
1.3.10 qRT-PCR	
1.3.11 Cell proliferation assay	
1.4 Results	15-20
1.4.1 Distinct glycosylation patterns between young and old epidermal stem cells	

1.4.2	Classes of lectins that differentially identified glycans in young and old stem cells	
1.4.3	Old epidermal stem cells display decreased mannose and increased Sia modifications	
1.4.4	Detection of age-related glycan changes in epidermal stem cells by flow cytometry using rHeltuba and rGal8N	
1.4.5	Up-regulation of sialyltransferase and mannosidase genes in old epidermal stem cells	
1.4.6	Recapitulation of old-type glycosylation pattern by overexpressing glycogenes causes functional impairment of epidermal stem cells <i>in vitro</i>	
1.5	Discussion	20-22
1.6	References	23-27
	<b>Chapter 2 :Fibulin-7, an extracellular matrix protein regulates the spatial niche of heterogeneous stem cell populations in the epidermis</b>	28-46
2.1	Abstract	28-29
2.2	Introduction	29-31
2.3	Experimental procedures	32-35
2.3.1	Mice	
2.3.2	BrdU treatment	
2.3.3	Whole-mount immunostaining of the mouse tail epidermis	
2.3.4	Tamoxifen injection	
2.3.5	FACS isolation of basal epidermal stem cells	
2.3.6	RNA isolation and RT-PCR	
2.3.7	RNA-sequencing analysis	
2.3.8	Glycan microarray	
2.3.9	Quantification	
2.4	Results	35-40

2.4.1	Loss of <i>Fbln7</i> leads to a transient increase in epidermal proliferation at younger age followed by a gradual decrease in proliferation overtime	
2.4.2	Loss of <i>Fbln7</i> leads a loss of fast-dividing stem cells and a disrupted epidermal stem cell compartments	
2.4.3	The loss of <i>Fbln7</i> affect the genes related to proliferation in the basal layer of the epidermis	
2.4.4	Fibulin-7 might bind with glycans, IGFP2, basement membrane components, and regulate the heterogeneous population of epidermal stem cells	
2.5	Discussion	40-41
2.6	References	42-46
	<b>FIGURES</b>	47-60

## ABBREVIATIONS

BCA assay: Bicinchoninic acid assay

BL: basal layer

BrdU: 5-Bromo-2'-deoxyuridine

CreER: Cyclization recombination- estrogen receptor

Cy3: Cyanine dye

ECM: Extracellular matrix

FACS: Fluorescence-activated cell sorting

*Fbln7*: Fibulin-7

GL: granular layer

H2B-GFP: Histone2B-green fluorescent protein

HFs: Hair follicles

HRP: horseradish peroxidase

IFE: Interfollicular epidermis

K: Keratin

LRCs: label-retaining cells

nLRCs: non- label retaining cells

PE: R-Phycoerythrin

Sia: Sialic acid

SL: spinous layer

TRE: Tetracycline response element

tTA: Tetracycline-dependent transactivator

## LIST OF FIGURES

**Figure 1.** Schematic representation of lectin microarray using freshly-isolated epidermal stem cells

**Figure 2.** Glycome analysis of young and old epidermal stem cells.

**Figure 3.** List of lectins significantly changed between young and old epidermal stem cells.

**Figure 4.** Detection of young and old epidermal stem cells by rHeltuba and rGal8N lectins.

**Figure 5.** The rHeltuba and rGal8N lectins differentially bind to freshly isolated young and old stem cells.

**Figure 6.** Gene expression analysis of glycosylation-related genes using RT2 Profiler PCR array.

**Figure 7.** Aging-associated glycogene overexpression leads to an impaired keratinocyte growth.

**Figure 8.** Different stem cell populations in the mouse skin.

**Figure 9.** H2B-GFP Tet-off system for identifying slow cycling cells.

**Figure 10.** *Fbln7* knockout strategy adapted from Tsunezumi et al., 2018

**Figure 11.** Whole-mount staining of tail epidermis in *Fbln7*<sup>-/-</sup> mice.

**Figure 12.** Lineage tracing of fast-dividing and slow cycling stem cells.

**Figure 13.** RNA-sequencing analysis of *Fbln7*<sup>-/-</sup> epidermal basal cells.

**Figure 14.** Identification of Fibulin-7 binding proteins.

**Figure 15.** Proposed model for the role of Fibulin-7 in maintenance of fast-dividing stem cells (scale region) in the mouse epidermis.

## Chapter 1

### Distinct glycosylation patterns during epidermal stem cell aging

#### 1.1 Abstract

Aging in the epidermis is marked by a gradual decline in barrier function, impaired wound healing, hair loss, and an increased risk of cancer. This could be due to age-related changes in the properties of epidermal stem cells or defective interactions with their microenvironment. Currently, no biochemical tools are available to detect and evaluate the aging of epidermal stem cells. The cellular glycosylation is involved in cell-cell communications and cell-matrix adhesions in various physiological and pathological conditions. Here I explored the changes of glycans in epidermal stem cells as a potential biomarker of aging. Using lectin microarray, I performed a comprehensive glycan profiling of freshly isolated epidermal stem cells from young and old mouse skin. Epidermal stem cells exhibited a significant difference in glycan profiles between young and old mice. In particular, the binding of a mannose-binder rHeltuba was decreased in old epidermal stem cells, whereas that of an  $\alpha$ 2-3 Sia-binder rGal8N increased. Gene expression analysis by quantitative PCR array further showed that these glycan changes were accompanied by the up-regulation of sialyltransferase and mannosidase genes in old epidermal stem cells. Hence, I demonstrated the age-related global alterations in cellular glycosylation patterns in epidermal stem cells. These glycan modifications detected by lectins may serve as molecular markers for aging, and further functional studies will lead us to a better understanding of the process of skin aging.

## 1.2 Introduction

The epidermis is the first barrier of our body that protects us from infection and dehydration. The epidermis consists of the interfollicular epidermis (IFE) and its appendages (hair follicles: HFs, sebaceous and sweat glands) and is replenished by distinct populations of stem cells [1] [2]. The IFE is renewed by stem cells located in the basal layer, which give rise to stratified squamous epithelium. HF stem cells reside in a specialized structure, called the bulge, and contribute to cyclic regeneration of HFs. Stem cells in the IFE and HFs are largely independent of each other during homeostasis, but they possess plasticity to change their fates in response to injury [1] [2]. The epidermis is separated from the dermis by the basement membrane enriched in the extracellular matrix, which regulates stem cell property and fates [3] [4].

An age-related decline in tissue regeneration and function could be attributed to an impaired stem cell function, a theory known as “stem cell aging” [5] [6]; however, it remains elusive what are the crucial drivers for aging at the cellular and molecular levels. An aged epidermis shows histological and functional changes, including a decrease in epidermal thickness, flattening of the epidermal-dermal junction [7] [8] [9] [10], impaired wound healing [11], decreased barrier function [2], increased risk of cancer [12] [5], hair loss [13] and lower success in epidermal engraftment [14]. Mutant mouse studies and transcriptome analyses have suggested that the age-related epidermal dysfunction could be due to defects in IFE and HF stem cells to interact with other cell types or extracellular matrix in skin [15] [16] [17] [13] [18] [11] [19]. However, changes in gene expression at the transcription level may not fully explain the molecular aspects of stem cell aging in skin.

Glycosylation is a reaction that proteins or lipids are modified with glycans [20]. The protein glycosylation involves stepwise addition and removal of glycans, primarily mediated by glycosyltransferases and glycosidases [21]. The presence of glycans determines the structure, stability, and localization of glycoproteins, which affect a wide variety of biological processes,

such as development [22], tumorigenesis [23] and inflammation [24]. Glycans are required for stem cell regulations by modulating signaling molecules that govern self-renewal and differentiation of stem cells [25]. As glycans are located at the cell surface, they have been utilized as biomarkers, e.g., pluripotent status of mouse embryonic stem cells [26] [27] [26] and human-induced pluripotent stem cells [28]. Given the role of glycans in diverse biological and biochemical processes, glycosylation might play an important role in the process of stem cell aging. However, the glycosylation state of stem cells in aged mammalian tissues remains largely uncharacterized.

The glycome analysis of tissue stem cells has been challenging, as tissue stem cells are rare and large amounts of samples are required for the structural analysis of glycans by mass spectrometry. Lectin microarray, a platform for high-throughput glycome analysis, enables a comprehensive glycan profiling even from a relatively small number of cells [29]. Lectins are a class of glycan-binding proteins that recognize various glycan structures [30]. In lectin microarrays, a series of lectins with various glycan binding specificities are immobilized on a glass slide [31]. Lectin-glycan interactions are quantitatively measured as fluorescent signals after incubation with fluorescence-labeled samples in the lectin microarray [29]. Using this technology, glycoproteins isolated from various biological samples can be utilized for glycome analysis without the liberation of glycans [32].

In our current study, I performed a comprehensive glycome analysis of IFE and HF stem cells in the old mouse skin by using lectin microarray consisting of 96 lectins with various glycan binding specificities [28]. I found that epidermal stem cells undergo global changes in their glycosylation patterns during aging, with decreased mannose and increased sialic acid (Sia) modifications.

## **1.3 Experimental Procedures**

### **1.3.1 Mice**

All animal procedures were conducted following animal experimentation guidelines approved by the Institutional Animal Experiment Committee at the University of Tsukuba. Young (2-month-old) and old (22-24-month-old) C57BL/6 mice were purchased from Charles River Laboratories or Japan SLC. Both male and female mice were used for experiments. All the experimental mice were housed in the Laboratory Animal Resource Center, University of Tsukuba prior to experiments.

### **1.3.2 Isolation of epidermal stem cells by flow cytometry**

Mouse dorsal and ventral skin were dissected and the subcutaneous and fat tissues were removed from the dermal side of the skin. The skin was incubated in 0.25% trypsin/versene overnight at 4°C and for 30 minutes at 37°C. The single cell solution was prepared by scraping the epidermis and subsequent filtering with strainers (70 µm, followed by 40 µm). Cells were stained with the following antibodies for 30 minutes on ice: CD34-biotin (1:50, eBioscience, San Diego, CA), Streptavidin-APC (1:100, BD Biosciences, San Jose, CA), α6-integrin-BUV395 (1:100, BD Biosciences, custom order) and Sca1-BV421 (1:100, BD Biosciences). The dead cells were excluded by staining with propidium iodide (Sigma-Aldrich, St. Louis, MO). Cell isolation was performed with FACS Aria (BD Biosciences) and the data were analyzed with the FlowJo software (BD, Franklin Lakes, NJ).

### **1.3.3 Membrane protein isolation and quantification**

Hydrophobic membrane protein fractions were prepared using the CelLytic MEM Protein Extraction kit (Sigma-Aldrich) following the manufacturer's protocols. Proteins were quantified using a micro BCA assay kit (Thermo Fisher Scientific, Waltham, MA).

#### **1.3.4 Lectin microarray**

The high-density lectin microarray was produced according to the method previously described [28]. The protein concentration was adjusted to 2 µg/ml with PBST [10 mM PBS (pH 7.4), 140 mM NaCl, 2.7 mM KCl, 1% Triton X-100] and was labeled with Cy3-N-hydroxysuccinimide ester (GE Healthcare). Cy3-labeled proteins were diluted with probing buffer [25 mM Tris-HCl (pH 7.5), 140 mM NaCl, 2.7 mM KCl, 1 mM CaCl<sub>2</sub>, 1 mM MnCl<sub>2</sub>, and 1% Triton X-100] to 0.5 µg/ml and were incubated with the lectin microarray at 20 °C overnight. Samples were washed with probing buffer for three times, and fluorescence images were captured using a Bio-Rex scan 200 evanescent-field activated fluorescence scanner (Rexxam Co. Ltd., Kagawa, Japan).

The lectin signals of triplicate spots were averaged for each sample and normalized relative to the mean value of 96 lectins. The mean normalized lectin microarray data were used for unsupervised clustering with the average linkage method using Cluster 3.0 software. The heat map with clustering was visualized using Java Treeview. Significant differences in lectin intensity were calculated by unpaired Student's t-test. The principal component analysis was performed by using the mean normalized signals and was generated using IBM SPSS Statistics software (IBM Japan, Ltd., Tokyo, Japan).

#### **1.3.5 Lectin blotting**

Recombinant lectins (rHeltuba, rGal8N) were prepared using *E. Coli* as previously described [28]. Lectins were conjugated with HRP by using the HRP labeling kit (Dojindo, Rockville, MD) at the concentration of 0.5 mg/ml, and adjusted to the final concentration for incubation at 0.1 µg/ml.

One microgram of proteins from each cell population was separated by SDS-PAGE on a 5-20% gel (Perfect NT Gel system, NTH-676HP, DRC, Tokyo, Japan) and transferred onto

polyvinylidene fluoride membranes (Millipore, Burlington, MA). After blocking the membrane in CarboFree blocking solution (Vector Laboratories, Burlingame, CA) for 1 hour at room temperature, it was incubated with HRP-conjugated lectins overnight at 4 °C. The signals were detected by using Western Lighting Plus (NEL104001EA, PerkinElmer, Waltham, MA). Lectin blot intensities were quantified using ImageJ software (National Institute of Health). The high-intensity band was selected for quantification. Statistical significance was calculated by unpaired Student's *t*-test (GraphPad Prism8 software).

### **1.3.6 Detection of lectin binding to epidermal stem cells by flow cytometry**

Recombinant lectins (rHeltuba, rGal8N) were labeled with R-Phycoerythrin (PE) using Phycoerythrin Labeling Kit - NH<sub>2</sub> (Dojindo) according to the manufacturer's protocol. The single cell solution was prepared as described above and resuspended in 1% BSA (Sigma-Aldrich, SLBV4985) without using the serum. Cells were stained with Lectin-PE for 1 hour at 4°C, at the following concentrations: 1 µg/ml for rHeltuba-PE and 10 µg/ml for rGal8N-PE. For the inhibition assays, 0.1M mannose (Sigma, D-(+)-Mannose, SLBP6438V) and 0.1M lactose monohydrate sugar (WDK2045, Wako Pure Chemical Industries, Ltd, Osaka, Japan) were used. After washing, cells were stained with antibodies for 30 minutes on ice and analyzed by FACS Aria (BD Biosciences). Student's *t*-tests were performed to compare lectin signal intensity of young versus old stem cells (GraphPad Prism8 software).

### **1.3.7 RT<sup>2</sup> profiler for mouse glycosylation PCR arrays**

Total RNAs were isolated using the RNeasy Micro kit (QIAGEN, Hilden, Germany), according to the manufacturer's protocol. The integrity of the isolated RNA was assessed by using RNA Pico Chips and Agilent 2100 bioanalyzer (Agilent Technologies, Santa Clara, CA). RNA samples with the RNA integrity number above 8 were used for further analysis. The

cDNA was synthesized from 50 ng of mRNA using the RT<sup>2</sup> PreAMP cDNA Synthesis Kit (QIAGEN, 330451), followed by pre-amplification using the pathway-specific primer mix for mouse glycosylation (QIAGEN, PBM-046Z).

The relative mRNA expressions of 84 genes regulating mouse glycosylation in young and old IFE stem cells were analyzed using RT<sup>2</sup> Profiler™ PCR Arrays (QIAGEN, PAMM-046Z) following the manufacturer's instructions. The cDNA template prepared above was mixed with RT<sup>2</sup> SYBR Green qPCR Master Mix (QIAGEN, 330501) and nuclease-free water. The cDNA mixture of 25µl was applied to each well of the PCR arrays that contain the preloaded primer mix for each gene. The real-time PCR amplification and detection were performed using a Bio-Rad CFX96 Touch™ Real-Time PCR Detection System (Bio-Rad, Hercules CA). Amplification cycle was used as following: activation of DNA Taq polymerase at 95°C for 10 minutes, followed by 40 cycles of denaturation at 95 °C for 15 seconds and annealing for 1 minute at 60 °C. The threshold cycle ( $C_t$ ) was used for PCR array quantification. The threshold values were set similarly across all the PCR array used in the analysis, and the baseline was defined by using the automated baseline option of the machine. Gene whose  $C_t$  cycle was more than 35 was set as undetectable.  $C_t$  values of three biological replicates from each young and old IFE stem cells obtained from the real-time PCR array analysis was used for the  $\Delta\Delta C_t$  –based fold-change calculations. For the data analysis, web-based PCR data analysis provided from the data analysis center of Qiagen was used. Samples were normalized using automatic normalization from the five housekeeping genes (*Actb*, *B2m*, *Gapdh*, *Gusb*, *Hsp90ab1*) in the PCR array. An appropriate correction was also made during the web-based data analysis for the preamplification step. Gene expression whose fold is greater than 1.5 were selected.

### **1.3.8 Mouse primary keratinocytes isolation and culture**

Mouse primary keratinocytes were isolated from two-day-old C57BL6/J mouse skin as previously reported (Lichti, Anders, & Yuspa, 2008). Keratinocytes were seeded on mitomycin-treated, mouse embryonic fibroblasts and grown in low-calcium E-medium (15% chelex-treated FBS, 0.05 mM CaCl<sub>2</sub>). Keratinocytes were used from passage 6-13 for the subsequent analysis.

### **1.3.9 Lentivirus production and infection**

Mouse cDNA encoding *Man1a*, *St3gal2*, *St6gall* or EGFP were cloned into CSII-CMV-MCS-IRES2-Bsd vector (RIKEN, Tsukuba, Japan) and transfected to 293T cells using lipofectamine 3000 (Thermo Fisher Scientific, Waltham, MA) together with packaging vectors pRSV-Rev, pMD2.G and pMDLg/pRRE (Addgene). The medium containing lentivirus was collected on day two and three post-transfection and concentrated using a Lenti-X concentrator (Takara Bio, Kusatsu, Shiga, Japan).

Mouse keratinocytes were seeded at 50,000 cells in a 24 well culture plate coated with collagen IV (Sigma). One day later, keratinocytes were infected with lentivirus along with 4 µg/mL polybrene for 16 hours. The 300 µl of medium containing 100 µl each of the glycoproteins (*Man1a*, *St3Gal2*, *St6gall*) or 300 µl of medium containing lenti-EGFP were used. The medium was changed after 16 hours and the infected keratinocytes were selected by using blasticidin at a concentration of 1 µg/ml.

### **1.3.10 qRT-PCR**

Mouse keratinocytes RNA was isolated using the RNeasy micro kit (QIAGEN) and real-time RT-PCR was performed using iTaq Universal SYBR green supermix (Bio-Rad, Hercules, California, USA) with the following primers; *Man1a* forward: 5'-

GAGACCCAGTCTTTGCCGAA -3', *Man1a* reverse: 5'- CGACACATGATGTTGACCCC -  
3', *St3gal2* forward: 5'- CCTAATGTGGATTGCCAGCG -3', *St3gal2* reverse: 5'-  
TCTGGACCTTCTCTTTGTCCA -3', *St6gal1* forward: 5'-  
GGGCACAAAACTACCATCCG -3', *St6gal1* reverse: 5'-  
TGATACCACTGCGGAATGTCT -3'.

### 1.3.11 Cell proliferation assay

Keratinocyte proliferation was measured by using the Cell-Counting Kit-8 (CCK-8, Dojindo, Japan) following the manufacturer's instructions. In brief, blasticidin-selected keratinocytes were seeded in triplicate in a collagen-IV coated flat-bottom 96-well plate at 2,000 cells/well. Keratinocytes were grown in the E-medium, and analyzed at 0, 1, 3, 5 days after infection. Ten micro liter of CCK-8 reagent was incubated for 2 hours and the absorption of the samples was measured at 450 nm using xMark microplate reader (BioRad).

For microscope analysis, blasticidin-selected keratinocytes were seeded at 5,000 cells/well in a collagen-IV coated 24-well plate. Images were acquired by using the Evos FL cell imaging system (Thermo Fisher Scientific, Waltham, MA) at indicated time points.

## 1.4 Results

### 1.4.1 Distinct glycosylation patterns between young and old epidermal stem cells

To analyze the glycosylation state of epidermal stem cells during aging, IFE and HF stem cells were isolated from wild-type C57BL/6 mice at 2 months (young,  $N=4$ ) and 22-24 months (old,  $N=3$ ) of age and subjected to lectin microarray (Figure 1a). IFE stem cells ( $\alpha6$ -integrin<sup>+</sup>/CD34<sup>-</sup>/Sca1<sup>+</sup>) and HF stem cells ( $\alpha6$ -integrin<sup>+</sup>/CD34<sup>+</sup>) were isolated by flow cytometry based on their differential expression of cell surface markers (Figure 1b and 1c). Hydrophobic fractions

containing membrane proteins were extracted. Protein amounts ranging from 15 to 30  $\mu\text{g}$  were obtained from 100,000~300,000 IFE or HF stem cells. Proteins were labeled with Cy3 and incubated with lectin microarray (Figure 1a).

The obtained signals were mean-normalized and subjected to unsupervised hierarchical clustering, followed by a heat map analysis. The hierarchical clustering showed that young and old samples were clustered separately, indicating their distinct glycosylation patterns (Figure 2a). Stem cells in different epidermal compartments, the IFE and HF, also showed differential glycosylation patterns, compatible with their distinct transcriptome signatures [33]. To further examine the correlation of each cell population, I performed principal component analysis of the mean normalized signals and showed that young and old epidermal stem cells were separated by principal component 1 and 2 (Figure 2b). Thus, these data suggest that mouse IFE and HF stem cells undergo global alterations in glycosylation during aging.

#### **1.4.2 Classes of lectins that differentially identified glycans in young and old stem cells**

For the identification of lectins that were differentially bound to glycan structures between young and old stem cells, statistical analysis was performed using the mean normalized signals obtained from lectin microarray. Several classes of lectins were significantly changed ( $p < 0.01$ ) between young and old stem cells (Figure 3) and I categorized them based on their glycan-binding specificities.

In the IFE, 13 lectins were significantly higher in young stem cells, whereas 12 lectins were higher in old stem cells (Figure 3a). The lectins enriched in young IFE stem cells included mannose-binding lectins (NPA, GNA, DBAI, rHeltuba, Heltuba) [28] [34], fucose-binding lectins (AAL, rAAL, rBC2LCN, rAOL) and O-glycan (Tn)-binding lectins (HPA, DBAIII). Consistently, it has been shown that high mannose type N-glycans were highly enriched in human embryonic stem cells [35], with a possible role in the maintenance of stemness. The

fucose ( $\alpha$ 1-2)-binding rBC2LCN has previously been identified as a lectin biomarker for undifferentiated pluripotent stem cells [28].

In contrast, the lectins enriched in old IFE stem cells included Sia-binding lectins (ACG, rACG, rGal8N) [36] [37], fucose ( $\alpha$ 1-6)-binding lectins (rPTL and LCA) and O-glycan (T antigen) binding lectins (MPA, Jacalin and HEA) (Figure 3a). Since sialylation has been implicated in the aging of muscle and fibroblasts [38] [37] [36], it might have an universal role in the process of aging. In HFs, 11 and 15 lectins showed significant enrichment in young and old stem cells, respectively (Figure 3b). Notably, lectins of similar functional classes were detected with significant differences in both IFE and HFs. Taken together, our lectin microarray analysis identified common sets of lectins that recognize age-dependent glycan changes in IFE and HF stem cells: decreased mannose-binding lectins and increased Sia-binding lectins during aging.

#### **1.4.3 Old epidermal stem cells display decreased mannose and increased Sia modifications**

To detect age-related glycan changes in epidermal stem cells, a mannose-binding rHeltuba and an  $\alpha$ 2-3Sia-binding rGal8N were selected as recombinant lectin probes for further analysis. Quantification of signals in lectin microarray confirmed significantly higher signals of rHeltuba in young stem cells compared with old stem cells both in the IFE and HFs (Figure 4a). In contrast, rGal8N showed higher signals in old stem cells than young stem cells (Figure 4b). These results were validated by lectin blotting. One microgram of membrane proteins was separated by SDS-PAGE and blotted with two lectins conjugated with horseradish peroxidase (HRP). The lectin blotting using rHeltuba showed decreased signals in old IFE and HF stem cells compared with young counterparts (Figure 4c), consistent with lectin microarray results. The major bands were detected at 80 and 110 kDa in young IFE, and at 45 and 60 kDa in young HF in addition to 80 and 110 kDa bands, suggesting the mannose modification in multiple

proteins (Figure 4c). In contrast, rGal8N showed higher signals in old stem cells compared with young stem cells and major bands around 60 and 80 kDa were detected (Figure 4d). Hence, the identified lectins, rHeltuba and rGal8N, successfully detected distinct glycosylation between young and old epidermal stem cells.

#### **1.4.4 Detection of age-related glycan changes in epidermal stem cells by flow cytometry using rHeltuba and rGal8N**

To test the ability of lectin-directed detection of glycans in living stem cells, I employed flow cytometry analysis in young and old stem cells using rHeltuba and rGal8N. Fluorescent-labeled lectins (rHeltuba and rGal8N) were incubated with freshly isolated epidermal stem cells from wild-type skin at 2 months (young,  $N=3$ ) or 22-24 months (old,  $N=3$ ) of age. Flow cytometry analysis using rHeltuba showed a higher peak of signals in young stem cells compared with old stem cells in both IFE and HFs (Figure 5a, upper graphs). Statistical analysis of the mean fluorescence intensity of rHeltuba signals showed a significant difference between young and old HF stem cells (Figure 5c). To verify the specificity of rHeltuba binding to stem cells, competition assays were performed by adding excess mannose during incubation of the lectin with epidermal stem cells. Indeed, the rHeltuba signals in both young and old epidermal stem cells were abrogated in the presence of mannose (Figure 5a, lower graphs), confirming that the lectin detected mannose modifications on the surface of stem cells.

Similar flow cytometry experiments with rGal8N, the  $\alpha 2$ -3Sia-binding lectin, IFE showed a shift toward the higher signal intensity in old stem cells compared with young stem cells (Figure 5b, upper left, and 5d, left). In the HFs, however, there were no significant differences in the rGal8N signal intensity between young and old stem cells (Figure 5b, upper right, and 5d, right). The signals of rGal8N were inhibited by lactose, confirming the specific binding of rGal8N to glycans. Taken together, these data indicate that both rHeltuba and rGal8N lectin

probes successfully detected glycan changes in freshly isolated IFE stem cells by flow cytometry.

#### **1.4.5 Up-regulation of sialyltransferase and mannosidase genes in old epidermal stem cells**

To address which enzymes are responsible for age-related glycosylation changes in epidermal stem cells, I performed gene expression analysis using RT<sup>2</sup> profiler PCR array of mouse glycosylation-related genes. RNAs isolated from IFE stem cells at 2 months (young, N=3) or 22-24 months (old, N=3) of age were used for quantitative PCR. Among 84 genes involved in the glycosylation pathway, 14 genes were  $\geq 1.5$  fold upregulated in old IFE stem cells, whereas 3 genes were  $\geq 1.5$  fold downregulated (Figure 6a). Among them, five genes were identified with statistically significant differences ( $p < 0.05$ ). Sialyltransferase genes (*St3gal2* and *St6gal1*) were upregulated in old IFE stem cells (Figures 6a and b), consistent with our lectin microarray (Figure 3). *St3gal2* catalyzes the transfer of Sia from cyclic monophosphate-Sia to  $\beta$ -galactosides and forms  $\alpha$ -2,3 sialylated glycoconjugates [20]. Similarly, *St6gal1* catalyzes the addition of Sia to a galactose-containing substrate and form  $\alpha$ -2,6 sialylated glycoconjugates [20]. I also found that mannosidase gene *Man1a* was increased in old stem cells (Figure 6b). *Man1a* is an  $\alpha$ -1,2 mannosidase and is responsible for the removal of mannose residues to initiate the complex-type N-glycan formation [20], which matches with the decreased signals of mannose-binding lectins in old IFE stem cells (Figures 3). Thus, glycan changes of epidermal stem cells during aging are possibly mediated by the changes in glycosyltransferase and glycosidase expressions with age.

#### **1.4.6 Recapitulation of old-type glycosylation pattern by overexpressing glycogenes causes functional impairment of epidermal stem cells *in vitro***

Finally, we addressed whether age-related glycan changes are a consequence of aging or causal to induce age-related phenotypes in epidermal stem cells. To mimic the glycosylation pattern

of old epidermal stem cells, we overexpressed three glycosyltransferases (*Man1a*, *St3gal2*, *St6gal1*) in primary epidermal keratinocytes, an *in vitro* model of epidermal stem cells, and modified cell surface glycans to aging-like status (Figure 7a). Successful gene overexpression and changes of glycosylation were evaluated by qRT-PCR (Figure 7b) and lectin-blotting (Figure 7c and 7d). The keratinocytes showed decreased mannose and increased Sia modifications (Figure 7c and 7d), which are similar to the glycosylation pattern of old epidermal stem cells *in vivo* (Figure 4). Overexpression of three glycosyltransferases resulted in significantly less ability to proliferate as compared to the control keratinocytes infected with EGFP, and detached from a dish within 5 days of culture (Figure 7e and 7f). The overexpression of *Man1a* alone showed milder effects than *St3gal2* or *St6gal1* alone (Figure 7f). These data indicate that age-related glycan changes may in part be responsible for a decline in the proliferation ability of epidermal stem cells during aging.

## 1.5 Discussion

*In vivo* sign of aging in the skin can be observed at the tissue and organismal levels; however, the molecular aspects of aging at the stem cell level remains elusive. In our current study, we performed a high-throughput lectin-based glycan profiling on murine epidermal stem cells and revealed their dynamic glycan alterations during aging. I propose a concept, “glycome shift” as a new molecular factor of epidermal stem cell aging (Figure 6c): high mannose-type N-glycans are globally replaced by  $\alpha$ 2-3/6 sialylated complex type N-glycans with age. The identified lectins, the mannose-binding rHeltuba, and the  $\alpha$ 2-3Sia-binding rGal8N can be used as probes to visualize, select or remove aged stem cells, with implications in future applications for regenerative therapy and diagnosis of skin aging. I also provide a proof of concept that our lectin microarray platform [32] can successfully analyze the glycome of adult tissue stem cells,

which are rare in tissue ( $\leq 1\%$  of total skin cells) and their biochemical properties are not well-characterized due to technical difficulties.

An aged skin exhibits declined wound healing ability, which is in part caused by impaired crosstalk between epidermal stem cells and dendritic epithelial T cells [11]. Given that several immune cells, including dendritic cells, have mannose-binding receptors in the epidermis [39], the decreased mannose in old IFE stem cells that I observed here (Figure 6c) could be associated with the defective stem cell-immune cell interaction in aged skin.

Our study showed an increase in  $\alpha 2-3$  and  $\alpha 2-6$  sialylation along with the expression of the corresponding sialyltransferase (*St3gal2* and *St6gal1*) in old IFE stem cells (Figure 6c). In agreement with our findings, sialylation was reported to be increased in the aged mouse muscle [38]. The upregulation of sialyltransferases has also been suggested as a potential aging marker in human, which shows a higher activity of *St6gal1* in the plasma of individuals above 80 years of age [40]. In addition, an  $\alpha 2-6$  sialylation and the expression of *St6gal1* were upregulated during epithelial to mesenchymal transition and tumor formation [41] [42]. By contrast,  $\alpha 2-3/6$  sialylation was reported to be decreased during senescence and aging of human dermal fibroblasts [37]. In human pluripotent or mesenchymal stem cells, a higher sialylation is associated with a greater potential of stem cells [28] [43] [44]. The observed differences in the sialylation patterns might be due to the differences in cell types, species or target proteins, indicating a diverse role of sialylation in the process of aging. Future studies using conditional knock-out or overexpression of differentially expressed glycosyltransferases in the mouse epidermis will directly address the role of sialylation in the context of epidermal stem cell aging. As glycosylation plays a critical role in cell-cell and cell-matrix interactions, the changes in glycans on the surface of epidermal stem cells might affect their ability to interact with neighboring stem cells, other cell types (e.g., fibroblasts, immune cells, blood vessels), basement membrane and signaling molecules, all of which are essential components for

maintaining the skin integrity. It will be interesting in the future to identify core proteins in which differential glycosylation takes place and to reveal the functional importance and biological meaning of glycosylation in age-related skin dysfunction.

## 1.6 References

1. Rognoni E, Watt FM. Skin Cell Heterogeneity in Development, Wound Healing, and Cancer. *Trends Cell Biol.* 2018;28(9):709-22. doi: 10.1016/j.tcb.2018.05.002. PubMed PMID: 29807713; PubMed Central PMCID: PMC6098245.
2. Gonzales KAU, Fuchs E. Skin and Its Regenerative Powers: An Alliance between Stem Cells and Their Niche. *Dev Cell.* 2017;43(4):387-401. Epub 2017/11/22. doi: 10.1016/j.devcel.2017.10.001. PubMed PMID: 29161590; PubMed Central PMCID: PMC6098245.
3. Watt FM, Fujiwara H. Cell-extracellular matrix interactions in normal and diseased skin. *Cold Spring Harb Perspect Biol.* 2011;3(4). Epub 2011/03/29. doi: 10.1101/cshperspect.a005124. PubMed PMID: 21441589; PubMed Central PMCID: PMC3062212.
4. Chermnykh E, Kalabusheva E, Vorotelyak E. Extracellular Matrix as a Regulator of Epidermal Stem Cell Fate. *Int J Mol Sci.* 2018;19(4). Epub 2018/03/28. doi: 10.3390/ijms19041003. PubMed PMID: 29584689; PubMed Central PMCID: PMC5979429.
5. López-Otín C, Blasco MA, Partridge L, Serrano M, Kroemer G. The Hallmarks of Aging. *Cell.* 2013;153(6):1194-217. doi: 10.1016/j.cell.2013.05.039.
6. Goodell MA, Rando TA. Stem cells and healthy aging. *Science.* 2015;350(6265):1199-204. Epub 2016/01/20. doi: 10.1126/science.aab3388. PubMed PMID: 26785478.
7. Giangreco A, Goldie SJ, Failla V, Saintigny G, Watt FM. Human skin aging is associated with reduced expression of the stem cell markers beta1 integrin and MCSP. *J Invest Dermatol.* 2010;130(2):604-8. Epub 2009/09/25. doi: 10.1038/jid.2009.297. PubMed PMID: 19776755.
8. Makrantonaki E, Zouboulis CC. Molecular mechanisms of skin aging: state of the art. *Ann N Y Acad Sci.* 2007;1119:40-50. Epub 2007/12/07. doi: 10.1196/annals.1404.027. PubMed PMID: 18056953.
9. Changarathil G, Ramirez K, Isoda H, Sada A, Yanagisawa H. Wild-type and SAMP8 mice show age-dependent changes in distinct stem cell compartments of the interfollicular epidermis. *PLoS One.* 2019;14(5):e0215908. Epub 2019/05/16. doi: 10.1371/journal.pone.0215908. PubMed PMID: 31091266; PubMed Central PMCID: PMC6519801.
10. Langton AK, Halai P, Griffiths CEM, Sherratt MJ, Watson REB. The impact of intrinsic ageing on the protein composition of the dermal-epidermal junction. *Mechanisms of Ageing and Development.* 2016;156:14-6. doi: <https://doi.org/10.1016/j.mad.2016.03.006>.
11. Keyes BE, Liu S, Asare A, Naik S, Levorse J, Polak L, et al. Impaired Epidermal to Dendritic T Cell Signaling Slows Wound Repair in Aged Skin. *Cell.* 2016;167(5):1323-38 e14.

doi: 10.1016/j.cell.2016.10.052. PubMed PMID: 27863246; PubMed Central PMCID: PMC5364946.

12. Adams PD, Jasper H, Rudolph KL. Aging-Induced Stem Cell Mutations as Drivers for Disease and Cancer. *Cell stem cell*. 2015;16(6):601-12. doi: 10.1016/j.stem.2015.05.002. PubMed PMID: 26046760.

13. Matsumura H, Mohri Y, Binh NT, Morinaga H, Fukuda M, Ito M, et al. Hair follicle aging is driven by transepidermal elimination of stem cells via COL17A1 proteolysis. *Science*. 2016;351(6273):aad4395. doi: 10.1126/science.aad4395. PubMed PMID: 26912707.

14. Piccin D, Morshead CM. Potential and pitfalls of stem cell therapy in old age. *Dis Model Mech*. 2010;3(7-8):421-5. Epub 2010/05/28. doi: 10.1242/dmm.003137. PubMed PMID: 20504968.

15. Rezvani HR, Ali N, Serrano-Sanchez M, Dubus P, Varon C, Ged C, et al. Loss of epidermal hypoxia-inducible factor-1 $\alpha$  accelerates epidermal aging and affects re-epithelialization in human and mouse. *Journal of Cell Science*. 2011;124(24):4172. doi: 10.1242/jcs.082370.

16. Watanabe M, Natsuga K, Nishie W, Kobayashi Y, Donati G, Suzuki S, et al. Type XVII collagen coordinates proliferation in the interfollicular epidermis. *eLife*. 2017;6:e26635. doi: 10.7554/eLife.26635.

17. Liu N, Matsumura H, Kato T, Ichinose S, Takada A, Namiki T, et al. Stem cell competition orchestrates skin homeostasis and ageing. *Nature*. 2019;568(7752):344-50. doi: 10.1038/s41586-019-1085-7.

18. Keyes BE, Segal JP, Heller E, Lien WH, Chang CY, Guo X, et al. Nfatc1 orchestrates aging in hair follicle stem cells. *Proc Natl Acad Sci U S A*. 2013;110(51):E4950-9. Epub 2013/11/28. doi: 10.1073/pnas.1320301110. PubMed PMID: 24282298; PubMed Central PMCID: PMC3870727.

19. Giangreco A, Qin M, Pinter JE, Watt FM. Epidermal stem cells are retained in vivo throughout skin aging. *Aging Cell*. 2008;7(2):250-9. doi: 10.1111/j.1474-9726.2008.00372.x. PubMed PMID: 18221414.

20. Varki A. In: nd, Varki A, Cummings RD, Esko JD, Freeze HH, Stanley P, et al., editors. *Essentials of Glycobiology*. Cold Spring Harbor (NY): Cold Spring Harbor Laboratory Press; 2009.

21. Spiro RG. Protein glycosylation: nature, distribution, enzymatic formation, and disease implications of glycopeptide bonds. *Glycobiology*. 2002;12(4):43r-56r. Epub 2002/06/04. doi: 10.1093/glycob/12.4.43r. PubMed PMID: 12042244.

22. Haltiwanger RS, Lowe JB. Role of Glycosylation in Development. *Annual Review of Biochemistry*. 2004;73(1):491-537. doi: 10.1146/annurev.biochem.73.011303.074043. PubMed PMID: 15189151.

23. Ohtsubo K, Marth JD. Glycosylation in cellular mechanisms of health and disease. *Cell*. 2006;126(5):855-67. doi: 10.1016/j.cell.2006.08.019. PubMed PMID: 16959566.
24. Varki A, Gagneux P. Biological Functions of Glycans. In: rd, Varki A, Cummings RD, Esko JD, Stanley P, Hart GW, et al., editors. *Essentials of Glycobiology*. Cold Spring Harbor (NY): Cold Spring Harbor Laboratory Press  
Copyright 2015-2017 by The Consortium of Glycobiology Editors, La Jolla, California. All rights reserved.; 2015. p. 77-88.
25. Nishihara S. Glycans in stem cell regulation: from *Drosophila* tissue stem cells to mammalian pluripotent stem cells. *FEBS Letters*. 2018;592(23):3773-90. doi: 10.1002/1873-3468.13167.
26. Muramatsu T, Muramatsu H. Carbohydrate antigens expressed on stem cells and early embryonic cells. *Glycoconjugate Journal*. 2004;21(1):41-5. doi: 10.1023/B:GLYC.0000043746.77504.28.
27. Adewumi O, Aflatoonian B, Ahrlund-Richter L, Amit M, Andrews PW, Beighton G, et al. Characterization of human embryonic stem cell lines by the International Stem Cell Initiative. *Nat Biotechnol*. 2007;25(7):803-16. Epub 2007/06/19. doi: 10.1038/nbt1318. PubMed PMID: 17572666.
28. Tateno H, Toyota M, Saito S, Onuma Y, Ito Y, Hiemori K, et al. Glycome diagnosis of human induced pluripotent stem cells using lectin microarray. *J Biol Chem*. 2011;286(23):20345-53. Epub 2011/04/08. doi: 10.1074/jbc.M111.231274. PubMed PMID: 21471226; PubMed Central PMCID: PMC3121447.
29. Kuno A, Uchiyama N, Koseki-Kuno S, Ebe Y, Takashima S, Yamada M, et al. Evanescent-field fluorescence-assisted lectin microarray: a new strategy for glycan profiling. *Nat Methods*. 2005;2(11):851-6. Epub 2005/11/10. doi: 10.1038/nmeth803. PubMed PMID: 16278656.
30. Hirabayashi J. Lectin-based structural glycomics: glycoproteomics and glycan profiling. *Glycoconj J*. 2004;21(1-2):35-40. Epub 2004/10/07. doi: 10.1023/B:GLYC.0000043745.18988.a1. PubMed PMID: 15467396.
31. Hirabayashi J, Yamada M, Kuno A, Tateno H. Lectin microarrays: concept, principle and applications. *Chem Soc Rev*. 2013;42(10):4443-58. Epub 2013/02/28. doi: 10.1039/c3cs35419a. PubMed PMID: 23443201.
32. Tateno H, Uchiyama N, Kuno A, Togayachi A, Sato T, Narimatsu H, et al. A novel strategy for mammalian cell surface glycome profiling using lectin microarray. *Glycobiology*. 2007;17(10):1138-46. Epub 2007/08/19. doi: 10.1093/glycob/cwm084. PubMed PMID: 17693441.
33. Joost S, Zeisel A, Jacob T, Sun X, La Manno G, Lonnerberg P, et al. Single-Cell Transcriptomics Reveals that Differentiation and Spatial Signatures Shape Epidermal and Hair Follicle Heterogeneity. *Cell Syst*. 2016;3(3):221-37.e9. Epub 2016/09/20. doi: 10.1016/j.cels.2016.08.010. PubMed PMID: 27641957; PubMed Central PMCID: PMC5052454.

34. Maupin KA, Liden D, Haab BB. The fine specificity of mannose-binding and galactose-binding lectins revealed using outlier motif analysis of glycan array data. *Glycobiology*. 2012;22(1):160-9. Epub 2011/08/31. doi: 10.1093/glycob/cwr128. PubMed PMID: 21875884; PubMed Central PMCID: PMC3230281.
35. An HJ, Gip P, Kim J, Wu S, Park KW, McVaugh CT, et al. Extensive determination of glycan heterogeneity reveals an unusual abundance of high mannose glycans in enriched plasma membranes of human embryonic stem cells. *Mol Cell Proteomics*. 2012;11(4):M111.010660. Epub 2011/12/08. doi: 10.1074/mcp.M111.010660. PubMed PMID: 22147732; PubMed Central PMCID: PMC3322563.
36. Sasaki N, Itakura Y, Toyoda M. Sialylation regulates myofibroblast differentiation of human skin fibroblasts. *Stem Cell Research & Therapy*. 2017;8(1):81. doi: 10.1186/s13287-017-0534-1.
37. Itakura Y, Sasaki N, Kami D, Gojo S, Umezawa A, Toyoda M. N- and O-glycan cell surface protein modifications associated with cellular senescence and human aging. *Cell & Bioscience*. 2016;6(1):14. doi: 10.1186/s13578-016-0079-5.
38. Hanisch F, Weidemann W, Großmann M, Joshi PR, Holzhausen H-J, Stoltenburg G, et al. Sialylation and muscle performance: sialic acid is a marker of muscle ageing. *PloS one*. 2013;8(12):e80520-e. doi: 10.1371/journal.pone.0080520. PubMed PMID: 24349002.
39. Wollenberg A, Mommaas M, Oppel T, Schottdorf EM, Gunther S, Moderer M. Expression and function of the mannose receptor CD206 on epidermal dendritic cells in inflammatory skin diseases. *J Invest Dermatol*. 2002;118(2):327-34. Epub 2002/02/14. doi: 10.1046/j.0022-202x.2001.01665.x. PubMed PMID: 11841552.
40. Catera M, Borelli V, Malagolini N, Chiricolo M, Venturi G, Reis CA, et al. Identification of novel plasma glycosylation-associated markers of aging. *Oncotarget*. 2016;7(7):7455-68. doi: 10.18632/oncotarget.7059. PubMed PMID: 26840264.
41. Lu J, Isaji T, Im S, Fukuda T, Hashii N, Takakura D, et al. beta-Galactoside alpha2,6-sialyltransferase 1 promotes transforming growth factor-beta-mediated epithelial-mesenchymal transition. *J Biol Chem*. 2014;289(50):34627-41. Epub 2014/10/26. doi: 10.1074/jbc.M114.593392. PubMed PMID: 25344606; PubMed Central PMCID: PMC4263869.
42. Swindall AF, Londoño-Joshi AI, Schultz MJ, Fineberg N, Buchsbaum DJ, Bellis SL. ST6Gal-I Protein Expression Is Upregulated in Human Epithelial Tumors and Correlates with Stem Cell Markers in Normal Tissues and Colon Cancer Cell Lines. *Cancer Research*. 2013;73(7):2368. doi: 10.1158/0008-5472.CAN-12-3424.
43. Hasehira K, Tateno H, Onuma Y, Ito Y, Asashima M, Hirabayashi J. Structural and quantitative evidence for dynamic glycome shift on production of induced pluripotent stem cells. *Mol Cell Proteomics*. 2012;11(12):1913-23. Epub 2012/10/02. doi: 10.1074/mcp.M112.020586. PubMed PMID: 23023295; PubMed Central PMCID: PMC3518133.

44. Wang Y-C, Stein JW, Lynch CL, Tran HT, Lee C-Y, Coleman R, et al. Glycosyltransferase ST6GAL1 contributes to the regulation of pluripotency in human pluripotent stem cells. *Scientific Reports*. 2015;5:13317. doi: 10.1038/srep13317  
<https://www.nature.com/articles/srep13317#supplementary-information>.

## Chapter 2

### **Fibulin-7, an extracellular matrix protein, regulates the spatial niche of heterogeneous stem cell populations in the epidermis**

#### **2.1 Abstract**

The inter-follicular epidermis is the first barrier of our body to protect us from infection and dehydration. Different models have been proposed in the mouse epidermis to explain possible heterogeneity within the basal layer. One model suggested that the mouse epidermis contains two distinct stem cell populations that divide at a different rate and reside in the spatially segregated, distinct niches. However, it remains largely unknown which factors regulate the localization and function of heterogeneous populations of stem cells in the epidermis. Extracellular matrix (ECM) is one of the critical components of the stem cell niche and provides structural and biochemical support for stem cells. Fibulin-7 (*Fbln7*), a fibulin family of ECM proteins, is known to play an essential role in the regulation of kidney calcification and odontoblasts differentiation by interacting with heparin and other ECM components. Here I show that Fibulin-7 is highly expressed in fast-dividing stem cells in the epidermis and functionally crucial for these cells to control their proliferation and long-term maintenance. The genetic ablation of *Fbln7* leads to a transient increase in epidermal proliferation at a younger age, followed by a gradual decrease in proliferation over time. This phenotype might be caused by the depletion of fast-dividing stem cells due to the over-proliferation of these cells, as supported by lineage tracing using *Slc1a3-CreER*. Interestingly, upon the loss of fast-dividing populations, slow-cycling stem cells marked by *Dlx-CreER* make ectopic clones in the fast-dividing region, indicating a possible compensation between different stem cell populations. Given that Fibulin-7 could potentially bind with glycans, IGFBP2, and basement membrane components, Fibulin-7 might act as a hub to create a specialized microenvironment

for fast-dividing stem cells and define the territorial segregation of different stem cell populations in the epidermis.

## **2.2 Introduction**

Tissue stem cells reside in a specialized microenvironment called a niche where they proliferate and differentiate for tissue turnover and repair [1]. Previous studies have proposed different components of stem cell niche in various mammalian tissues, which comprise neighboring cells, growth factors, extracellular matrix (ECM) and physical forces [2] [3] [4] [5] [6] [7]. The niche controls quiescence, activation, and differentiation of stem cells by sending signals or via physical interactions [8]. A breach in the stem cell niche leads to a defect in tissue repairs [9], tumorigenesis [10], and degenerative diseases including aging [11] [12] [13]. It is of great importance to understand the cellular and molecular components of stem cell niche, which can provide basic knowledge on regenerative therapy and modeling diseases [9].

The skin is the first barrier of the body that protects against infection and dehydration. It comprises of two main layers separated by a basement membrane rich in extracellular matrix (ECM): (1) the epidermis, an outermost layer of skin, consisting of the inter-follicular epidermis (IFE) and its associated appendages such as hair follicles (HFs), sebaceous glands and sweat glands (Figure 8a) [14] [15] [16] and (2) the dermis, an underlying mesenchymal compartment mainly composed of fibroblasts and ECM.

The IFE is replenished by stem cells present in the basal layer, which can differentiate and move upwards to form the spinous, the granular and the terminally-differentiated cornified layers [17]. Different populations of stem cells in the IFE have been reported, yet there is no unified model to explain the possible heterogeneity within the basal layer of the IFE [15]. One model proposed that the basal layer consists of two distinct populations of stem cells that divide at a different rate and reside at distinct regions of the IFE [18] [19]. The proposed two

populations of stem cells were most evident in the tail IFE, which shows characteristic structures, interscale and scale [18] (Figure 8b). The interscale IFE is replenished by slow-cycling stem cells that undergo K10<sup>+</sup> orthokeratotic differentiation, whereas the scale IFE is populated by fast-dividing stem cells that undergo K31<sup>+</sup> parakeratotic differentiation characterized by the lack of granular layer and retention of the nucleus in the cornified layer [18] [19]. Sada et al. showed by lineage tracing that slow-cycling and fast-dividing stem cells were marked by Dlx1- and Slc1a3-CreER, respectively, and both populations retain long-term stem cell potential in vivo (Figure 8b) [18]. This is also supported by Lgr6-CreER mediated lineage tracing, showing that cells in the interscale IFE regenerate their own regions, but not the scale [20]. Two stem cell populations act independently during homeostasis, but they could breach their territorial segregation and contribute to each other's territory in response to injury. A study further identified Eddard and Wnt/ $\beta$ -catenin signaling as a regulator of interscale/scale lineages in the tail IFE, as its mutant mice change the size of the scale and interscale [18]. The interscale region of the mouse IFE was more prone to the formation of basal cell carcinoma as compared to scale region, suggesting the functional importance of stem cell heterogeneity in scale and interscale [21]. However, it is largely unknown how their division frequency and distinct localization are regulated between slow-cycling and fast-dividing stem cells in the IFE. Cell-cell and cell-ECM matrix are an integral component of the stem cell niche [2]. Proliferating cells in the basal layer contact with the basement membrane (ECM) through the cell surface integrins [22] and the ECM component has been implicated in controlling proliferation, cell polarity, anchorage and fate of epidermal stem cells through the cell-surface transmembrane integrins [23]. ECM also plays a vital role in sequestering various growth factors and cytokines [24]. Dysregulation of the ECM components in the stem cell niche can lead to a defect in tissue regenerative capacity and a diseased state such as tumorigenesis and aging [25]. The loss of the ECM component, including the  $\beta$ 1-integrin, has been reported in

the misalignment of the spindle orientation affecting the cell-cell adhesion [26]. Type XVII collagen (COL17) is associated with junctional epidermolysis [27] and aging [28, 29]. Hair follicle stem cells in each region express uniquely defined ECM and create a niche for muscle[30] and nerves [31], suggesting that the diverse composition of ECM may be playing an essential role in the stem cell compartmentalization.

I hypothesize that differential ECM components between slow-cycling and fast-dividing IFE stem cells may create their specific environments and play a role in their regulation. To address this hypothesis, I selected one ECM molecule Fibulin-7, which was found to be highly expressed in fast-dividing stem cells[19]. Fibulins are groups of secreted glycoproteins associated with the ECM structure of the basement membrane and connective tissue fibers [32]. They have different binding motifs modulators which enable them to interact with other ECM constituents and to mediate the cellular processes or tissue remodeling [33]. Fibulin-7 is the newest member of the Fibulin family ECM protein, which acts as a modular protein with different binding motifs [34]. Fibulin-7 has been reported to interact with heparin and ECM component such as fibronectin, fibulin-1, and dentin sialophosphoprotein [34]. Recently a study from our group reported that *Fbln7* is found to be expressed in the renal tubular epithelium and promotes renal calcification in mice [35]. However, the role of Fibulin-7 in the adult mouse skin remains unknown.

In my current study, I show that the loss of *Fbln7* leads to epidermal hyperproliferation, followed by the gradual loss of fast-dividing stem cell population. The *Fbln7* mutant slow-cycling population presented ectopic clones in the fast-dividing region, suggesting a breached in the spatial segregation of the two stem cell populations. Given its molecular function as an adhesion molecule with a capacity to interact with cell surface receptors and other ECM proteins [34] [35], I propose Fibulin-7 as a niche factor for defining the compartmentalized, heterogeneous stem cell populations in the mouse IFE.

## **2.3 Experimental procedures**

### **2.3.1 Mice**

Animal experiments were conducted according to the guidelines approved by the Institutional Animal Experiment Committee at the University of Tsukuba. The generation of mice deficient in the fibulin-7 gene (*Fbln7*<sup>-/-</sup>) was previously reported [35], and *Fbln7* wild-type (*Fbln7*<sup>+/+</sup>), *Fbln7* heterozygous (*Fbln7*<sup>+/-</sup>) and *Fbln7*<sup>-/-</sup> mice were used in this study. The K5-tTA[52]/pTRE-H2B-GFP/K14-CreER[53]/Rosa26tdTomato(The Jackson Laboratory, no. 007905) quadruple transgenic mice were used for the isolation of LRCs and non-LRCs epidermal stem cells [18]. For lineage-tracing experiment, *Dlx1*-CreER (C57BL6) (The Jackson Laboratory, no. 014551) or *Slc1a3*-CreER (C57BL6) (The Jackson Laboratory, no. 012586) mice were crossed with *Fbln7*<sup>+/-</sup> mice to generate *Fbln7*<sup>+/-</sup>;*Dlx1*-CreER and *Fbln7*<sup>+/-</sup>;*Slc1a3*-CreER, respectively. and further with Rosa-tdTomato (The Jackson Laboratory, no. 007905) reporter mice. For RNA-sequencing of basal epidermal stem cells, *Fbln7*<sup>+/+</sup> and *Fbln7*<sup>-/-</sup> mice at the age of 2 months and 1 year were used. All the experimental mice were kept on a 12h/12h light/dark cycle in the Laboratory Animal Resource Center at the University of Tsukuba before the experiments. Both sexes of mice were used for all analyses.

### **2.3.2 BrdU treatment**

For checking the proliferative cells, BrdU (5-Bromo-2'-deoxyuridine; Sigma-Aldrich, B5002) was administered in drinking water (0.8 mg/ml) for two days before sacrifice.

### **2.3.3 Whole-mount immunostaining of the mouse tail epidermis**

Tail whole-mount samples were collected from mice and processed as described before [18]. Primary antibodies were used at the following dilutions: rabbit anti-caspase-3, active (cleaved) form (1:100, Millipore, AB3623, polyclonal), rat anti-BrdU (1:300, Abcam, ab6326

monoclonal), rat anti- $\beta$ 4-integrin (1:100, BD Biosciences), mouse anti-K10 (1:100, BioLegend, 904301, monoclonal or 1:100, Abcam, ab9026, monoclonal), guinea pig anti-K31 (1:100, PROGEN Biotechnik, GP-hHa1, polyclonal). Secondary antibodies (Alexa 488 or Alexa 546, Invitrogen) were used at 1:200 dilution. Primary mouse antibodies were blocked with the MOM kit (Vector Laboratories). The samples were counterstained with Hoechst (Sigma, B2261) for 1 hour and mounted. For BrdU staining, tail whole-mount pieces were blocked with serum and incubated for 1 hour at 37°C in 2N HCl, then washed and stained with BrdU antibody. The stained whole-mount epidermis was mounted and observed under a confocal microscope (Zeiss LSM 700). The images were captured and analyzed with a ZEN 2010 software. All pictures are shown as projected Z-stack images and viewed from the basal side.

#### **2.3.4 Tamoxifen injection**

For lineage tracing of fast-dividing stem cells (Slc1a3-CreER) and slow-cycling stem cells (Dlx1-CreER), mice were injected with Tamoxifen (Sigma) intraperitoneally with a single dose of 25  $\mu$ g and 50  $\mu$ g per g body weight, respectively, at postnatal day (PD)49.

#### **2.3.5 FACS isolation of basal epidermal stem cells**

Mouse dorsal and ventral skin were dissected, and the subcutaneous and fat tissues were removed from the dermal side of the skin. The skin was incubated in 0.25% trypsin/versene overnight at 4°C and for 30 minutes at 37°C. The single-cell solution was prepared by scraping the epidermis and subsequent filtering with strainers (70  $\mu$ m, followed by 40  $\mu$ m). Cells were stained with the following antibodies for 30 minutes on ice: CD34-biotin (1:50, eBioscience, San Diego, CA), Streptavidin-APC (1:100, BD Biosciences, San Jose, CA),  $\alpha$ 6-integrin-BUV395 (1:100, BD Biosciences, custom order) and Sca1-BV421 (1:100, BD Biosciences).

Dead cells were excluded by staining with propidium iodide (Sigma-Aldrich, St. Louis, MO). Cell isolation was performed with FACS Aria (BD Biosciences), and the data were analyzed with the FlowJo software (BD, Franklin Lakes, NJ).

### **2.3.6 RNA isolation and RT-PCR**

Total RNA was prepared from the different populations of FACS sorted epidermal cells using the RNeasy micro kit (Qiagen). Reverse transcription was performed with Superscript III (Invitrogen), followed by PCR amplification using the following primers : *Gapdh*; 5'-ACTGCCACCCAGAAGACTGT-3' and 5'-GATGCAGGGATGATGTTCT-3' and *Fbln7*; 5'-GAGGAGGCTTCCAGTGTGTC-3' and 5'-AATGGAAGGAGATGGTCTTGG-3'. GAPDH gene was used for normalization. The *Fbln7* transcripts in basal layer LRCs was set to 1.

### **2.3.7 RNA-sequencing analysis**

RNA sequencing was performed using *Fbln7*<sup>+/+</sup> and *Fbln7*<sup>-/-</sup> mice (N=2 per genotype). Basal epidermal stem cells were directly sorted into TRIzol (Ambion, 10296028) and submitted to Tsukuba i-Laboratory LLP, the University of Tsukuba for further analysis. RNA sequencing was performed using the next generation sequencing (NGS) platform. Data analysis of the RNA sequencing was performed using CLC genomics 10 software (Qiagen). Genes with "zero" expression values were excluded after normalization. The remaining genes that showed 2-fold up- or downregulation in the basal epidermal stem cells of *Fbln7*<sup>+/+</sup> and *Fbln7*<sup>-/-</sup> mice were selected and gene ontology analysis was performed by using online tools VENNY 2.1 (<https://bioinfogp.cnb.csic.es/tools/venny/>) and PANTHER (<http://www.pantherdb.org>).

### 2.3.8 Glycan microarray

Glycan array was produced similarly as described previously[54]. Fibulin-7 protein (R&D) was labeled with Cy3 by dissolving it in the probing buffer [25 mM Tris-HCl (pH 7.5), 140 mM NaCl, 2.7 mM KCl, 1 mM CaCl<sub>2</sub>, 1 mM MnCl<sub>2</sub>, and 1% Triton X-100] at a concentration of 1 or 10 µg/ml. One hundred microliters of each concentration were applied to each well of the glycan array and incubated at 20 °C overnight. Samples were washed with probing buffer for three times, and fluorescence images were captured using a Bio-Rex scan 200 evanescent-field activated fluorescence scanner (Rexxam Co. Ltd., Kagawa, Japan). The intensity of each glycol-conjugate spot was determined by actual signal intensity minus background value. The Fibulin-7 signals from the triplicate spots were averaged and normalized to the highest signal intensity among all the 98 glycoconjugates on the glycan array.

### 2.3.9 Quantification

Lineage tracing quantification of tdTomato positive clones was manually counted from at least 16 interscale and scale structures from the projected Z-stack images. The number of mice is shown in the figure legends. Data are expressed as means ± standard error of the mean (S.E.M.).

## 2.4 Results

### 2.4.1 Loss of *Fbln7* leads to a transient increase in epidermal proliferation at younger age followed by a gradual decrease in proliferation overtime

The previous microarray has shown that *Fbln7* expression is enriched in fast-dividing cells in the IFE [18]. To confirm the expression pattern of *Fbln7* by qRT-PCR, I isolated different epidermal compartments by using the quadruple transgenic mice (K14-CreER/Rosa-tdTomato/K5-tTA/pTRE-H2B-GFP) [18](Figure 9a and 9b). In this system, a green

fluorescent protein (GFP) is transcribed in the skin epidermis under the K5 promoter in the absence of tetracycline (doxycycline; doxy). The treatment of doxy prevents the transcription of GFP. During doxy chase, cells dilute GFP protein by divisions, and only cells divided less frequently retain the GFP label and, therefore, can be identified as label-retaining cells (LRCs). The preferential labeling of the IFE is achieved by K14-CreER-driven tdTomato expression after injecting a low dose of Tamoxifen. By combining with cell surface markers,  $\alpha 6$ -integrin and CD34, 5 IFE cell populations were separated by using fluorescence activated cell sorting (FACS): basal layer (BL) LRCs, BL nLRCs, spinous layer (SL) LRCs, SL nLRCs, and granular layer (GL) (Figure 9c). I found that the expression of *Fbln7* was 5.8 -fold higher in BL nLRCs (fast-dividing cells) as compared to BL LRCs. (Figure 9d). Thus, I confirmed that *Fbln7* mRNA is highly expressed in fast-dividing population in the basal layer of IFE.

The enriched expression of *Fbln7* might indicate its possible role as a niche factor for fast-dividing stem cells. To understand the role of *Fbln7* during epidermal homeostasis, I analyzed the proliferation, differentiation, and apoptosis in the skin IFE of *Fbln7*<sup>-/-</sup> mice (Figure 10 and [35]). I employed the BrdU labeling at 2-months and 1-year-old for the three different genotypes: *Fbln7*<sup>+/+</sup> (WT), *Fbln7*<sup>+/-</sup>, and *Fbln7*<sup>-/-</sup> mice. In the WT tail IFE, BrdU positive cells were enriched in the scale region where fast-dividing stem cells reside. At 2 months, *Fbln7*<sup>-/-</sup> mice showed increased proliferation as compared to the control WT mice, especially in the scale (Figure 11a). By 1 year of age, *Fbln7*<sup>+/-</sup> and *Fbln7*<sup>-/-</sup> mice showed a decline in its proliferation (Figure 11a). These results indicate that the deletion of *Fbln7* leads to a transient increase in epidermal proliferation at a younger age, followed by a gradual decrease in proliferation over time.

Given that *Fbln7* is important for odontoblast differentiation, I addressed if the deletion of *Fbln7* also affects the differentiation of IFE. By staining with differentiation markers, Keratin 31 (K31) and Keratin 10 (K10) in the whole-mount IFE, no apparent differences were found

in the differentiation pattern between the *Fbln7*<sup>+/+</sup> and *Fbln7*<sup>-/-</sup> in any time points examined (Figure 11b).

There are reports that when cells are detached from ECM they undergo apoptosis [36]. To address the possible role of Fibulin-7 in apoptosis regulation, I stained cleaved caspase-3 antibodies and found that there was no presence of apoptotic cells in the IFE of the *Fbln7*<sup>-/-</sup> mice (Figure 11c). From these results, I conclude that the loss of *Fbln7* affects proliferation but not the differentiation nor apoptosis. There is a previous report that *Fbln7* is expressed in the hair follicles [37], but I could not detect any phenotype in the hair cycles or hair morphology.

#### **2.4.2 Loss of *Fbln7* results in a loss of fast-dividing stem cells and disrupted epidermal stem cell compartments**

The misregulation of stem cell proliferation leads to increased DNA damage, impaired wound healing, tumorigenesis and aging [38] [39, 40]. To address if the over-proliferation of IFE stem cells observed in *Fbln7* deficiency affects long-term stem cell potential in vivo, I performed single-cell labeling and lineage tracing of fast-dividing and slow-cycling stem cells in the IFE. I introduced Slc1a3- and Dlx1-CreER, as markers of fast-dividing and slow-cycling stem cells, respectively on a *Fbln7*<sup>-/-</sup> background (Figure 12a). Mice were sacrificed at 1-week, 3-months, and one-year post-Tamoxifen injection, and tdTomato positive clones were analyzed. In *Fbln7*<sup>+/+</sup> mice, fast-dividing stem cells marked by Slc1a3-CreER were maintained in the scale region, whereas the slow-cycling stem cells marked by Dlx1-CreER were maintained in the interscale for up to 1 year as previously shown by Sada et al [19]. In the *Fbln7*<sup>+/-</sup> and *Fbln7*<sup>-/-</sup> mice, Slc1a3-CreER-positive clones showed no apparent differences at 1-week and 3-month chases (Figure 12a and 12c). At 1-year-chase, *Fbln7*<sup>-/-</sup> mice showed significantly fewer clones in the fast-dividing scale region as compared with the WT mice. The fast-dividing scale region

of the 1-year-chased WT mice had 2~3 tdTomato positive clones, whereas the *Fbln7*<sup>-/-</sup> mice had only 1 or no clones at all (Figure 12a and 12c). This result suggests that the fast-dividing stem cells gradually lost their long-term stem cell ability in the absence of *Fbln7*.

Next, we performed lineage tracing of slow-cycling stem cells by using *Dlx1*-CreER. I could only analyze the clones from *Fbln7*<sup>+/+</sup> and *Fbln7*<sup>+/-</sup>, as the genes *Dlx1* and *Fbln7* are located on the same chromosome (57.33 Mb apart). The analysis of slow-cycling stem cells (*Dlx1*-CreER<sup>+</sup> clones) at 1 week showed no apparent differences (Figure 12b). At 3 months and 1-year chases, tdTomato-positive clones were found to be ectopically present in the fast-dividing scale region in *Fbln7*<sup>+/-</sup> mice (Figure 12b and 12c). The presence of ectopic clones is reminiscent of the epidermal injury, in which *Dlx1*<sup>+</sup> or *Slc1a3*<sup>+</sup> marked clones migrated and expanded to other stem cell's compartment [18]. Thus, the loss of *Fbln7* leads to a defect in the compartmentalization and long-term maintenance of IFE stem cells.

### **2.4.3 The loss of *Fbln7* affects the genes related to proliferation in the basal layer of the epidermis**

The *Fbln7* KO phenotypes suggest possible roles of Fibulin-7 in creating a distinct niche for the fast-dividing stem cells and controlling their proper location and division frequency. To analyze the downstream genes and signaling pathways affected by the loss of Fibulin-7, I performed RNA-sequencing of IFE stem cells in *Fbln7*<sup>-/-</sup> mice (Figure 13a). The basal epidermal ( $\alpha 6$ -integrin<sup>+</sup>/CD34<sup>-</sup>/Sca1<sup>+</sup>) cells were isolated using FACS from the WT control and *Fbln7*<sup>-/-</sup> mice at two-month of age. To examine the transcriptomic changes associated with the deletion of *Fbln7*, I compared the genes that were greater than two-fold differentially expressed between the *Fbln7*<sup>+/+</sup> and *Fbln7*<sup>-/-</sup> mice. I found that 628 genes were differentially expressed (Figure 13b), 325 genes were downregulated, and 303 genes were upregulated in the *Fbln7*<sup>-/-</sup> mice. Gene ontology (GO) analyses revealed that the GO categories related to cell-

cycle, cell-division, regulation of transcription, and cellular response to DNA stimuli were upregulated in the *Fbln7*<sup>-/-</sup> mice (Figure 13b). Among the upregulated genes, many of the genes were involved in the regulation of cell division: *Cks1b* (cyclin-dependent kinase sub-regulatory-1) is a prognostic marker for multiple myeloma [41]. *Cdca3* is a cell cycle regulator in which its overexpression promotes oral cancer by preventing cell cycle arrest [42]. *Ect2* (epithelial cell transforming sequence 2) is reported to play an important role in cell division and its dysregulation causes tumorigenesis [43] (Ulke, H. M., et al.). These results suggest that the loss of Fibulin-7 might affect sequestration of cytokines and growth factors in fast-dividing stem cells, and may explain a more proliferative phenotype in the *Fbln7*<sup>-/-</sup> mice.

#### **2.4.4 Fibulin-7 might bind with glycans, IGFP2, basement membrane components, and regulate the heterogeneous population of epidermal stem cells.**

Previously it was shown that Fibulin-7 could bind with heparan sulfate and could mediate the deposition of calcium phosphate in the renal tubular epithelium[35]. Thus, Fibulin-7 could also interact with other glycans and regulate the fast-dividing stem cells. There are studies that have shown the importance of glycans in the maintenance of stem cells (Berger, R. P., et al.2016). To examine the biochemical role of Fibulin-7 in interacting with other glycans, I performed a glycan-binding experiment using a glycan microarray. I found that Fibulin-7 could bind with other glycans including heparin, asialo, agalacto-transferrin, and sialyl 3-lactose glycans (Figure 14a). Transferrin (CD71) serves as a marker for human-keratinocytes [44] and the low expression of CD71 in keratinocytes were shown to be more potent for reconstructing the epidermis[44]. It is possible that Fibulin-7 might regulate stem cell proliferation and maintenance by binding with the transferrin and inhibiting its expression in the cell surface. Previous work in our laboratory has identified the possible binding molecules of Fibulin-7, which were co-precipitated with Fibulin-7 (Tsunezumi et al., unpublished, Figure 13b and 13c).

By comparing the list of binding molecules with the microarray gene lists[18], I found several molecules that could potentially interact with Fibulin-7 and were highly expressed in fast-dividing stem cell population. They include IGFBP2, Fibulin-1, Fibronectin, Laminin  $\alpha$ 5, Perlecan, Nidogen-1, Desmoglein-1, Tenascin, Dermcidin, Neuropilin-2, Fibrillin-2, BMP1, Corneodesmosin, Tissue-type plasminogen activator, Canstatin, etc (Figure 14b and 14c). IGFBP2 is reported to be important for the maintenance of epidermal stem cells and also during the initiation of basal cell carcinoma [45]. Fibronectin is known to inhibit differentiation of human keratinocytes and is an ECM used for coating the culture plate for culturing stem cells [46]. Nidogen-1 is an important component of the basement membrane of the skin and the lack of Nidogen-1 prevents the basement membrane assembly [47]. Desmoglein-1 is required for epidermal differentiation and morphogenesis [48]. Tenascin interacts with epidermal growth factor receptors (EGFR) regulating stem cell proliferation during wound healing[49]. These results suggest that Fibulin-7 might interact with glycans, growth factors, and basement membrane components to create a distinct microenvironment for the fast-dividing stem cell population.

## **2.5 Discussion**

Fibulin-7 is the newest member of the Fibulin family of secreted glycoproteins with a possible role in the developing teeth[34], a mediator of calcium phosphate deposition in the renal tubes[35], negative regulator of monocyte and macrophage migration [50], and an antiangiogenic factor that interacts with matrix proteins, growth factors, and receptors [51]. In my current study, I demonstrate that Fibulin-7 regulates compartmentalization and proliferation of fast-dividing stem cells in the skin IFE. The loss of fast-dividing stem cells by the deletion of Fibulin-7 presented a similar phenotype as injury observed in the previous study where another population migrated and interconvert, suggesting the plasticity of two stem cell

populations in different models of niche disruption. It will also be interesting to look into the role of Fibulin-7 during injury repair at 1-year-old mice when the proliferation decreases in *Fbln7* <sup>-/-</sup> mice. In addition, it will be interesting to examine the contribution of Fibulin-7 in inflammatory skin diseases with parakeratosis, such as psoriasis or actinic keratosis, and whether the cells are more susceptible to inflammatory signals.

As a biochemical function of Fibulin-7, I propose that Fibulin-7 might create a specialized microenvironment for fast-dividing stem cells by binding with glycans like transferrin[44] and/or by sequestering growth factors and cytokines including IGFBP2 [45], thereby regulating the bioavailability of these factors (Figure 15). It could also play an important role in maintaining a proper assembly of the basement membrane components, such as Nidogen-1, Fibronectin, Desmoglein-1, and Tenascin as supported by Fibulin-7 binding experiments. Alternatively, Fibulin-7 may modulate the binding between the components of basement membranes and their integrin receptors. Currently, the exact mechanism by which Fibulin-7 maintains the two distinct stem cell populations is not known and further studies are needed. The recapitulation of the *in vivo* environment is important for the translation of fundamental stem cell biology discovery for stem cell therapy. My study suggests that Fibulin-7 might be an important component for the replication of the *in vivo* niche in the *in vitro* culture of IFE stem cells.

## 2.6 Reference

1. Morrison SJ, Spradling AC. Stem Cells and Niches: Mechanisms That Promote Stem Cell Maintenance throughout Life. *Cell*. 2008;132(4):598-611. doi: 10.1016/j.cell.2008.01.038.
2. Ferraro F, Celso CL, Scadden D. Adult stem cells and their niches. *Adv Exp Med Biol*. 2010;695:155-68. Epub 2011/01/12. doi: 10.1007/978-1-4419-7037-4\_11. PubMed PMID: 21222205; PubMed Central PMCID: PMC4020242.
3. Crane GM, Jeffery E, Morrison SJ. Adult haematopoietic stem cell niches. *Nature Reviews Immunology*. 2017;17:573. doi: 10.1038/nri.2017.53.
4. Rompolas P, Greco V. Stem cell dynamics in the hair follicle niche. *Semin Cell Dev Biol*. 2014;25-26:34-42. Epub 2013/12/24. doi: 10.1016/j.semcdb.2013.12.005. PubMed PMID: 24361866; PubMed Central PMCID: PMC3988239.
5. Mills JC, Gordon JI. The intestinal stem cell niche: there grows the neighborhood. *Proc Natl Acad Sci U S A*. 2001;98(22):12334-6. Epub 2001/10/25. doi: 10.1073/pnas.231487198. PubMed PMID: 11675485; PubMed Central PMCID: PMC60050.
6. Bentzinger CF, Wang YX, Dumont NA, Rudnicki MA. Cellular dynamics in the muscle satellite cell niche. *EMBO reports*. 2013;14(12):1062-72. doi: 10.1038/embor.2013.182.
7. Conover JC, Notti RQ. The neural stem cell niche. *Cell Tissue Res*. 2008;331(1):211-24. Epub 2007/10/09. doi: 10.1007/s00441-007-0503-6. PubMed PMID: 17922142.
8. Pennings S, Liu KJ, Qian H. The Stem Cell Niche: Interactions between Stem Cells and Their Environment. *Stem Cells International*. 2018;2018:3. doi: 10.1155/2018/4879379.
9. Wagers Amy J. The Stem Cell Niche in Regenerative Medicine. *Cell Stem Cell*. 2012;10(4):362-9. doi: <https://doi.org/10.1016/j.stem.2012.02.018>.
10. Plaks V, Kong N, Werb Z. The cancer stem cell niche: how essential is the niche in regulating stemness of tumor cells? *Cell Stem Cell*. 2015;16(3):225-38. Epub 2015/03/10. doi: 10.1016/j.stem.2015.02.015. PubMed PMID: 25748930; PubMed Central PMCID: PMC4355577.
11. Chakkalakal JV, Jones KM, Basson MA, Brack AS. The aged niche disrupts muscle stem cell quiescence. *Nature*. 2012;490(7420):355-60. Epub 2012/10/02. doi: 10.1038/nature11438. PubMed PMID: 23023126; PubMed Central PMCID: PMC3605795.
12. Latchney SE, Calvi LM. The aging hematopoietic stem cell niche: Phenotypic and functional changes and mechanisms that contribute to hematopoietic aging. *Semin Hematol*. 2017;54(1):25-32. Epub 2017/01/17. doi: 10.1053/j.seminhematol.2016.10.001. PubMed PMID: 28088984; PubMed Central PMCID: PMC444432.
13. Gonzales KAU, Fuchs E. Skin and Its Regenerative Powers: An Alliance between Stem Cells and Their Niche. *Dev Cell*. 2017;43(4):387-401. Epub 2017/11/22. doi:

10.1016/j.devcel.2017.10.001. PubMed PMID: 29161590; PubMed Central PMCID: PMC5797699.

14. Rognoni E, Watt FM. Skin Cell Heterogeneity in Development, Wound Healing, and Cancer. *Trends in Cell Biology*. 2018;28(9):709-22. doi: <https://doi.org/10.1016/j.tcb.2018.05.002>.

15. Oinam L, Changarathil G, Ngo YX, Yanagisawa H, Sada A. Chapter Two - Epidermal stem cell lineages. In: Perez-Moreno M, editor. *Advances in Stem Cells and their Niches*. 3: Elsevier; 2019. p. 31-72.

16. Simpson CL, Patel DM, Green KJ. Deconstructing the skin: cytoarchitectural determinants of epidermal morphogenesis. *Nat Rev Mol Cell Biol*. 2011;12(9):565-80. Epub 2011/08/24. doi: 10.1038/nrm3175. PubMed PMID: 21860392; PubMed Central PMCID: PMC3280198.

17. Gomez C, Chua W, Miremedi A, Quist S, Headon DJ, Watt FM. The interfollicular epidermis of adult mouse tail comprises two distinct cell lineages that are differentially regulated by Wnt, Edaradd, and Lrig1. *Stem Cell Reports*. 2013;1(1):19-27. Epub 2013/09/21. doi: 10.1016/j.stemcr.2013.04.001. PubMed PMID: 24052938; PubMed Central PMCID: PMC3757744.

18. Sada A, Jacob F, Leung E, Wang S, White BS, Shalloway D, et al. Defining the cellular lineage hierarchy in the interfollicular epidermis of adult skin. *Nature Cell Biology*. 2016;18(6):619-31. doi: <http://dx.doi.org/10.1038/ncb3359>. PubMed PMID: 1791907262.

19. Kretschmar K, Weber C, Driskell RR, Calonje E, Watt FM. Compartmentalized Epidermal Activation of  $\beta$ -Catenin Differentially Affects Lineage Reprogramming and Underlies Tumor Heterogeneity. *Cell Reports*. 2016;14(2):269-81. doi: <https://doi.org/10.1016/j.celrep.2015.12.041>.

20. Sánchez-Danés A, Hannezo E, Larsimont JC, Liagre M, Youssef KK, Simons BD, et al. Defining the clonal dynamics leading to mouse skin tumour initiation. *Nature*. 2016;536(7616):298-303. Epub 2016/07/28. doi: 10.1038/nature19069. PubMed PMID: 27459053; PubMed Central PMCID: PMC5068560.

21. Breitkreutz D, Koxholt I, Thiemann K, Nischt R. Skin basement membrane: the foundation of epidermal integrity--BM functions and diverse roles of bridging molecules nidogen and perlecan. *Biomed Res Int*. 2013;2013:179784. Epub 2013/04/16. doi: 10.1155/2013/179784. PubMed PMID: 23586018; PubMed Central PMCID: PMC3618921.

22. Chermnykh E, Kalabusheva E, Vorotelyak E. Extracellular Matrix as a Regulator of Epidermal Stem Cell Fate. *Int J Mol Sci*. 2018;19(4). Epub 2018/03/28. doi: 10.3390/ijms19041003. PubMed PMID: 29584689; PubMed Central PMCID: PMC5979429.

23. Taipale J, Keski-Oja J. Growth factors in the extracellular matrix. *Faseb j*. 1997;11(1):51-9. Epub 1997/01/01. doi: 10.1096/fasebj.11.1.9034166. PubMed PMID: 9034166.

24. Watt FM, Fujiwara H. Cell-Extracellular Matrix Interactions in Normal and Diseased Skin. *Cold Spring Harbor Perspectives in Biology*. 2011;3(4).
25. Petridou NI, Skourides PA. A ligand-independent integrin  $\beta 1$  mechanosensory complex guides spindle orientation. *Nature Communications*. 2016;7(1):10899. doi: 10.1038/ncomms10899.
26. Fine JD, Bruckner-Tuderman L, Eady RA, Bauer EA, Bauer JW, Has C, et al. Inherited epidermolysis bullosa: updated recommendations on diagnosis and classification. *J Am Acad Dermatol*. 2014;70(6):1103-26. Epub 2014/04/03. doi: 10.1016/j.jaad.2014.01.903. PubMed PMID: 24690439.
27. Watanabe M, Natsuga K, Nishie W, Kobayashi Y, Donati G, Suzuki S, et al. Type XVII collagen coordinates proliferation in the interfollicular epidermis. *Elife*. 2017;6. Epub 2017/07/12. doi: 10.7554/eLife.26635. PubMed PMID: 28693719; PubMed Central PMCID: PMC5505703.
28. Liu N, Matsumura H, Kato T, Ichinose S, Takada A, Namiki T, et al. Stem cell competition orchestrates skin homeostasis and ageing. *Nature*. 2019;568(7752):344-50. Epub 2019/04/05. doi: 10.1038/s41586-019-1085-7. PubMed PMID: 30944469.
29. Fujiwara H, Ferreira M, Donati G, Marciano DK, Linton JM, Sato Y, et al. The basement membrane of hair follicle stem cells is a muscle cell niche. *Cell*. 2011;144(4):577-89. Epub 2011/02/22. doi: 10.1016/j.cell.2011.01.014. PubMed PMID: 21335239; PubMed Central PMCID: PMC3056115.
30. Cheng CC, Tsutsui K, Taguchi T, Sanzen N, Nakagawa A, Kakiguchi K, et al. Hair follicle epidermal stem cells define a niche for tactile sensation. *Elife*. 2018;7. Epub 2018/10/26. doi: 10.7554/eLife.38883. PubMed PMID: 30355452; PubMed Central PMCID: PMC6226291.
31. Timpl R, Sasaki T, Kostka G, Chu ML. Fibulins: a versatile family of extracellular matrix proteins. *Nat Rev Mol Cell Biol*. 2003;4(6):479-89. Epub 2003/06/05. doi: 10.1038/nrm1130. PubMed PMID: 12778127.
32. Kobayashi N, Kostka G, Garbe JHO, Keene DR, Bächinger HP, Hanisch F-G, et al. A Comparative Analysis of the Fibulin Protein Family: BIOCHEMICAL CHARACTERIZATION, BINDING INTERACTIONS, AND TISSUE LOCALIZATION. *Journal of Biological Chemistry*. 2007;282(16):11805-16. doi: 10.1074/jbc.M611029200.
33. de Vega S, Iwamoto T, Nakamura T, Hozumi K, McKnight DA, Fisher LW, et al. TM14 is a new member of the fibulin family (fibulin-7) that interacts with extracellular matrix molecules and is active for cell binding. *J Biol Chem*. 2007;282(42):30878-88. Epub 2007/08/19. doi: 10.1074/jbc.M705847200. PubMed PMID: 17699513.
34. Tsunozumi J, Sugiura H, Oinam L, Ali A, Thang BQ, Sada A, et al. Fibulin-7, a heparin binding matricellular protein, promotes renal tubular calcification in mice. *Matrix Biology*. 2018;74:5-20. doi: <https://doi.org/10.1016/j.matbio.2018.04.014>.

35. Kim S-H, Turnbull J, Guimond S. Extracellular matrix and cell signalling: the dynamic cooperation of integrin, proteoglycan and growth factor receptor. 2011;209(2):139. doi: 10.1530/joe-10-0377.
36. Donati G, Proserpio V, Lichtenberger BM, Natsuga K, Sinclair R, Fujiwara H, et al. Epidermal Wnt/ $\beta$ -catenin signaling regulates adipocyte differentiation via secretion of adipogenic factors. *Proceedings of the National Academy of Sciences*. 2014;111(15):E1501-E9. doi: 10.1073/pnas.1312880111.
37. Clarke MF, Fuller M. Stem cells and cancer: two faces of eve. *Cell*. 2006;124(6):1111-5. Epub 2006/03/28. doi: 10.1016/j.cell.2006.03.011. PubMed PMID: 16564000.
38. Liu JC, Lerou PH, Lahav G. Stem cells: balancing resistance and sensitivity to DNA damage. *Trends Cell Biol*. 2014;24(5):268-74. Epub 2014/04/12. doi: 10.1016/j.tcb.2014.03.002. PubMed PMID: 24721782; PubMed Central PMCID: PMC4342985.
39. Changarathil G, Ramirez K, Isoda H, Sada A, Yanagisawa H. Wild-type and SAMP8 mice show age-dependent changes in distinct stem cell compartments of the interfollicular epidermis. *PLoS One*. 2019;14(5):e0215908. Epub 2019/05/16. doi: 10.1371/journal.pone.0215908. PubMed PMID: 31091266; PubMed Central PMCID: PMC6519801.
40. Zhan F, Colla S, Wu X, Chen B, Stewart JP, Kuehl WM, et al. CKS1B, overexpressed in aggressive disease, regulates multiple myeloma growth and survival through SKP2- and p27Kip1-dependent and -independent mechanisms. *Blood*. 2007;109(11):4995-5001. doi: 10.1182/blood-2006-07-038703.
41. Uchida F, Uzawa K, Kasamatsu A, Takatori H, Sakamoto Y, Ogawara K, et al. Overexpression of cell cycle regulator CDCA3 promotes oral cancer progression by enhancing cell proliferation with prevention of G1 phase arrest. *BMC Cancer*. 2012;12(1):321. doi: 10.1186/1471-2407-12-321.
42. Ulke HM, Mutze K, Lehmann M, Wagner DE, Heinzelmann K, Günther A, et al. The oncogene ECT2 contributes to a hyperplastic, proliferative lung epithelial cell phenotype in IPF. *American Journal of Respiratory Cell and Molecular Biology*. 0(ja):null. doi: 10.1165/rcmb.2019-0047OC. PubMed PMID: 31145635.
43. Metral E, Bechetoille N, Demarne F, Rachidi W, Damour O.  $\alpha 6$  Integrin ( $\alpha 6$ (high))/Transferrin Receptor (CD71)(low) Keratinocyte Stem Cells Are More Potent for Generating Reconstructed Skin Epidermis Than Rapid Adherent Cells. *Int J Mol Sci*. 2017;18(2). Epub 2017/01/31. doi: 10.3390/ijms18020282. PubMed PMID: 28134816; PubMed Central PMCID: PMC5343818.
44. Villani RM, Adolphe C, Palmer J, Waters MJ, Wainwright BJ. Patched1 Inhibits Epidermal Progenitor Cell Expansion and Basal Cell Carcinoma Formation by Limiting Igfbp2 Activity. *Cancer Prevention Research*. 2010;3(10):1222. doi: 10.1158/1940-6207.CAPR-10-0082.

45. Adams JC, Watt FM. Fibronectin inhibits the terminal differentiation of human keratinocytes. *Nature*. 1989;340(6231):307-9. doi: 10.1038/340307a0.
46. Nischt R, Schmidt C, Mirancea N, Baranowsky A, Mokkapati S, Smyth N, et al. Lack of Nidogen-1 and -2 Prevents Basement Membrane Assembly in Skin-Organotypic Coculture. *Journal of Investigative Dermatology*. 2007;127(3):545-54. doi: <https://doi.org/10.1038/sj.jid.5700562>.
47. Getsios S, Simpson CL, Kojima S-i, Harmon R, Sheu LJ, Dusek RL, et al. Desmoglein 1-dependent suppression of EGFR signaling promotes epidermal differentiation and morphogenesis. *The Journal of Cell Biology*. 2009;185(7):1243. doi: 10.1083/jcb.200809044.
48. Lu P, Takai K, Weaver VM, Werb Z. Extracellular Matrix Degradation and Remodeling in Development and Disease. *Cold Spring Harbor Perspectives in Biology*. 2011;3(12).
49. Sarangi PP, Chakraborty P, Wahl L, Yamada Y. Adhesion protein Fibulin-7 (Fbln7) regulate differentiation and polarisation of human monocytes and macrophages. *The Journal of Immunology*. 2017;198(1 Supplement):143.5.
50. Ikeuchi T, de Vega S, Forcinito P, Doyle AD, Amaral J, Rodriguez IR, et al. Extracellular Protein Fibulin-7 and Its C-Terminal Fragment Have In Vivo Antiangiogenic Activity. *Scientific Reports*. 2018;8(1):17654. doi: 10.1038/s41598-018-36182-w.
51. Diamond I, Owolabi T, Marco M, Lam C, Glick A. Conditional Gene Expression in the Epidermis of Transgenic Mice Using the Tetracycline-Regulated Transactivators tTA and rTA Linked to the Keratin 5 Promoter. *Journal of Investigative Dermatology*. 2000;115(5):788-94. doi: <https://doi.org/10.1046/j.1523-1747.2000.00144.x>.
52. Tumber T, Guasch G, Greco V, Blanpain C, Lowry WE, Rendl M, et al. Defining the epithelial stem cell niche in skin. *Science*. 2004;303(5656):359-63. Epub 2003/12/13. doi: 10.1126/science.1092436. PubMed PMID: 14671312; PubMed Central PMCID: PMC2405920.
53. Tateno H, Mori A, Uchiyama N, Yabe R, Iwaki J, Shikanai T, et al. Glycoconjugate microarray based on an evanescent-field fluorescence-assisted detection principle for investigation of glycan-binding proteins. *Glycobiology*. 2008;18(10):789-98. doi: 10.1093/glycob/cwn068. PubMed PMID: 18633134.

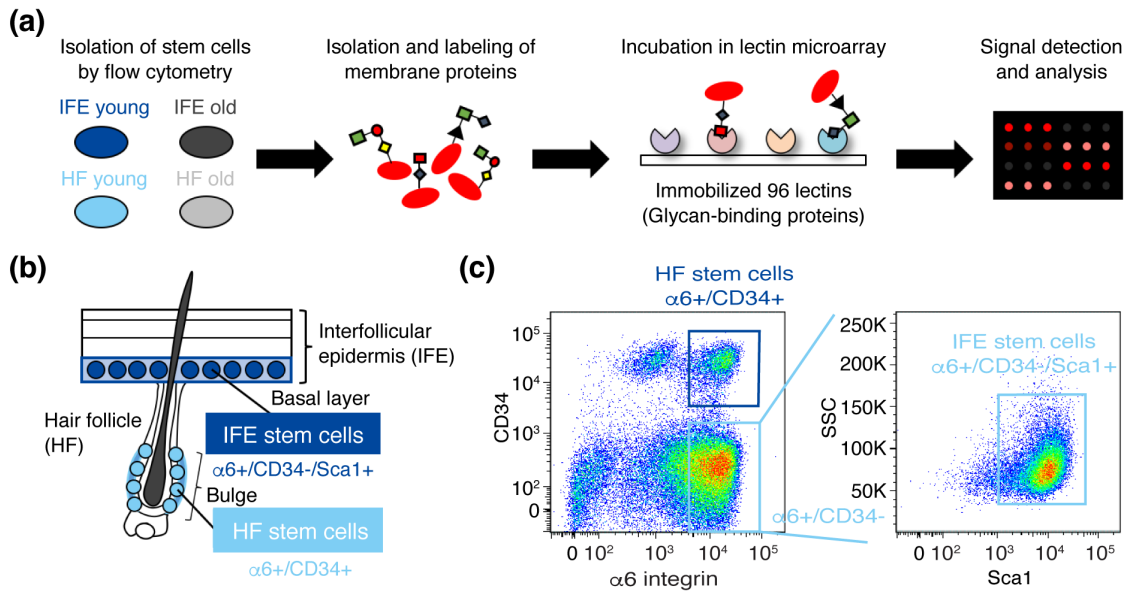


**Figure 1.** Schematic representation of lectin microarray using freshly-isolated epidermal stem cells. (a) Schematic representation of lectin microarray analysis. Cell membrane proteins are isolated, fluorescently-labeled and incubated with lectin microarray, in which 96 lectins are immobilized on glass slides. The lectin-glycan interactions are measured and quantified as signal intensities obtained from each lectin spot. (b) Schematic representation of epidermal cell types in mouse skin and cell surface markers used. (c) Flow cytometry dot plot and sorting gates for the isolation of epidermal skin subpopulations. Interfollicular epidermal (IFE) stem cells are defined as  $\alpha 6$ -integrin<sup>+</sup>/CD34<sup>-</sup>/Sca1<sup>+</sup>, and hair follicles (HF) stem cells are defined as  $\alpha 6$ -integrin<sup>+</sup>/CD34<sup>+</sup>.

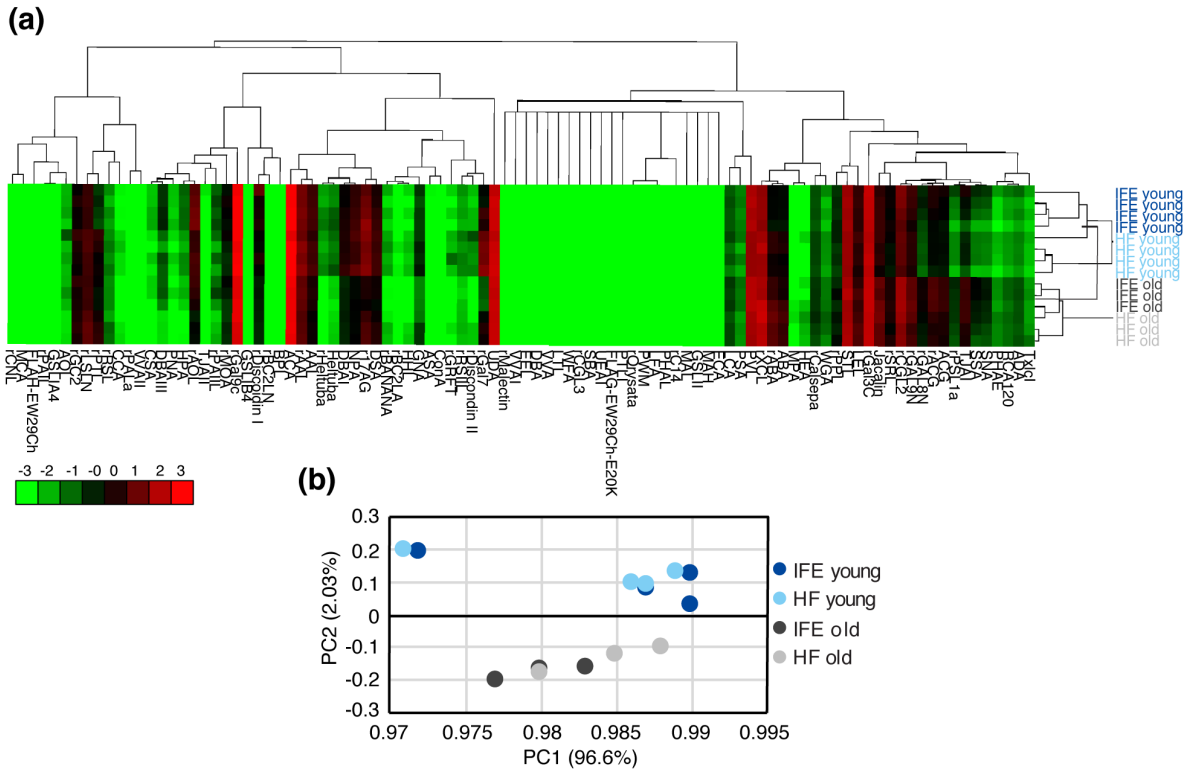


**Figure 2.** Glycome analysis of young and old epidermal stem cells. (a) Heat map and hierarchical clustering of lectin microarray signals. Each row represents different stem cell populations isolated from an individual mouse ( $N=4$  for young mice,  $N=3$  for old mice). Ninety-six lectins are shown on columns. (b) Principal component analysis of the mean normalized signals obtained from lectin microarray. A scatter plot for principal component (PC) 1 and 2 is shown. Each dot represents the sample derived from an individual mouse. Different cell types are indicated by color.

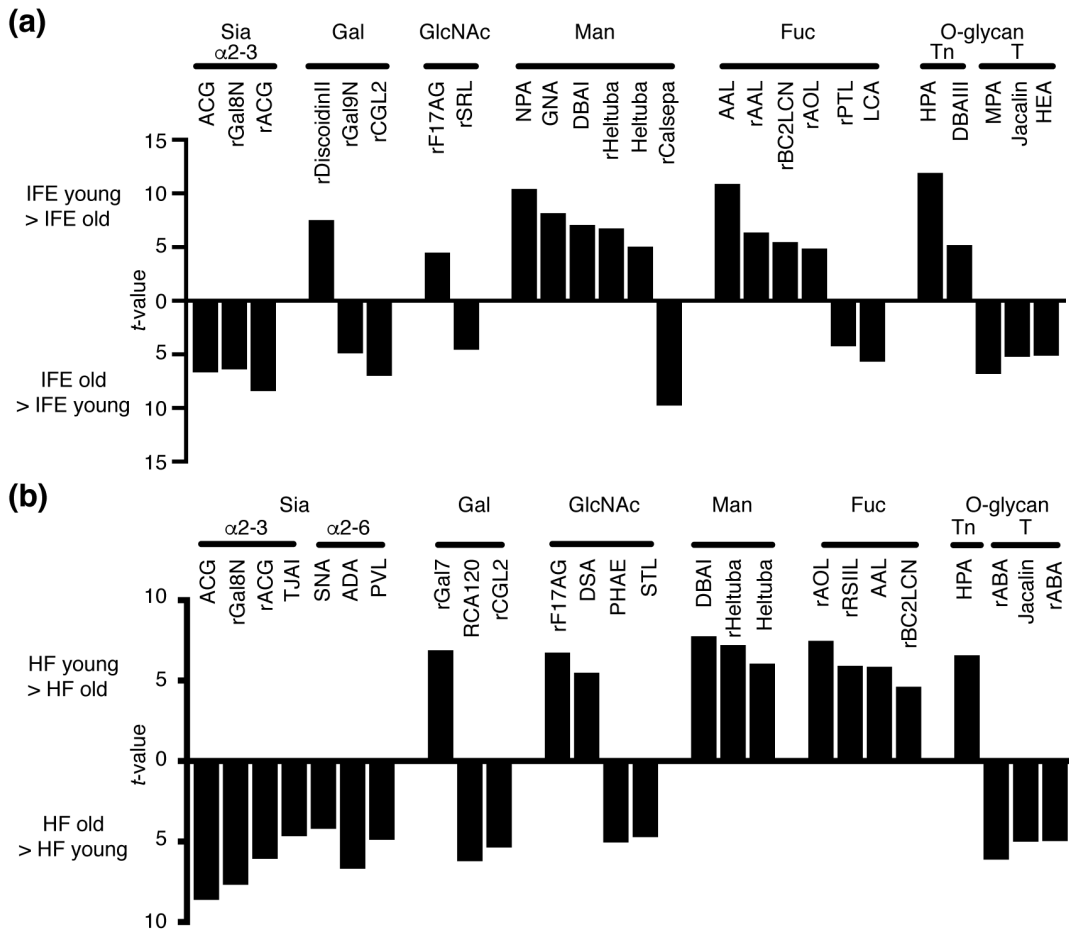


**Figure 3.** List of lectins significantly changed between young and old epidermal stem cells. (a, b) Lectins bound differentially to the young or old interfollicular epidermis (IFE) (a) and hair follicles (HF) (b). Statistically-significant differences are calculated by unpaired Student's t-test and  $p < 0.01$  are selected. Lectins are categorized based on their binding specificities. Data are shown with t-values.

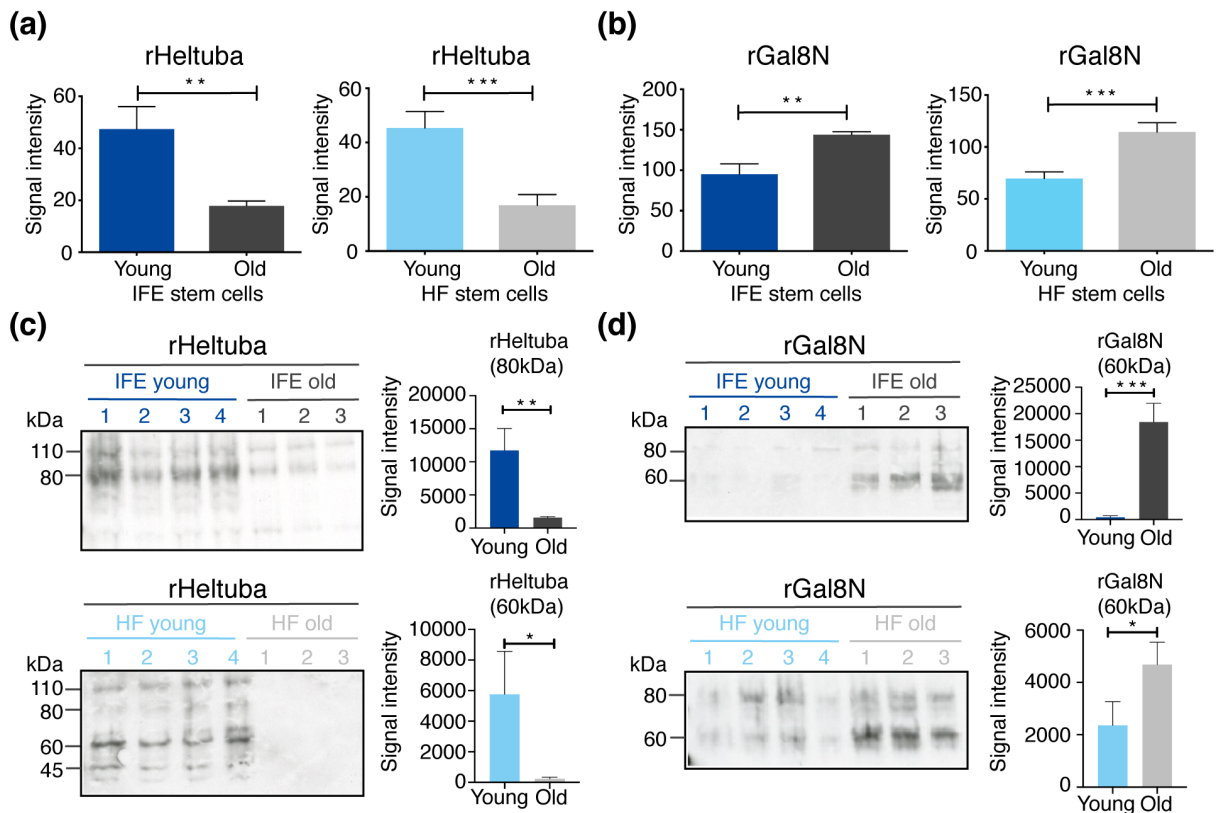


**Figure 4.** Detection of young and old epidermal stem cells by rHeltuba and rGal8N lectins. (a, b) Signal intensities of rHeltuba (Mana1-3Man, Mana1-6Man) (a) and rGal8N ( $\alpha$ 2-3Sia) (b) in the lectin microarray are shown. The lectin signals of individual mice are averaged and normalized to the average of 96 lectins.  $N=4$  for young mice,  $N=3$  for old mice. Data are shown as means  $\pm$  SD. Student's t-test. \*\*\*,  $p < 0.001$ . \*\*,  $p < 0.01$ . \*,  $p < 0.05$ . (c, d) Lectin blotting using the horseradish peroxidase (HRP)-labeled lectins, rHeltuba (c) and rGal8N (d). Young and old stem cells in the interfollicular epidermis (IFE) and hair follicles are used.  $N=4$  for young mice,  $N=3$  for old mice. One microgram of protein from a single mouse is applied in each lane. The signal intensities of bands with indicated size are quantified.

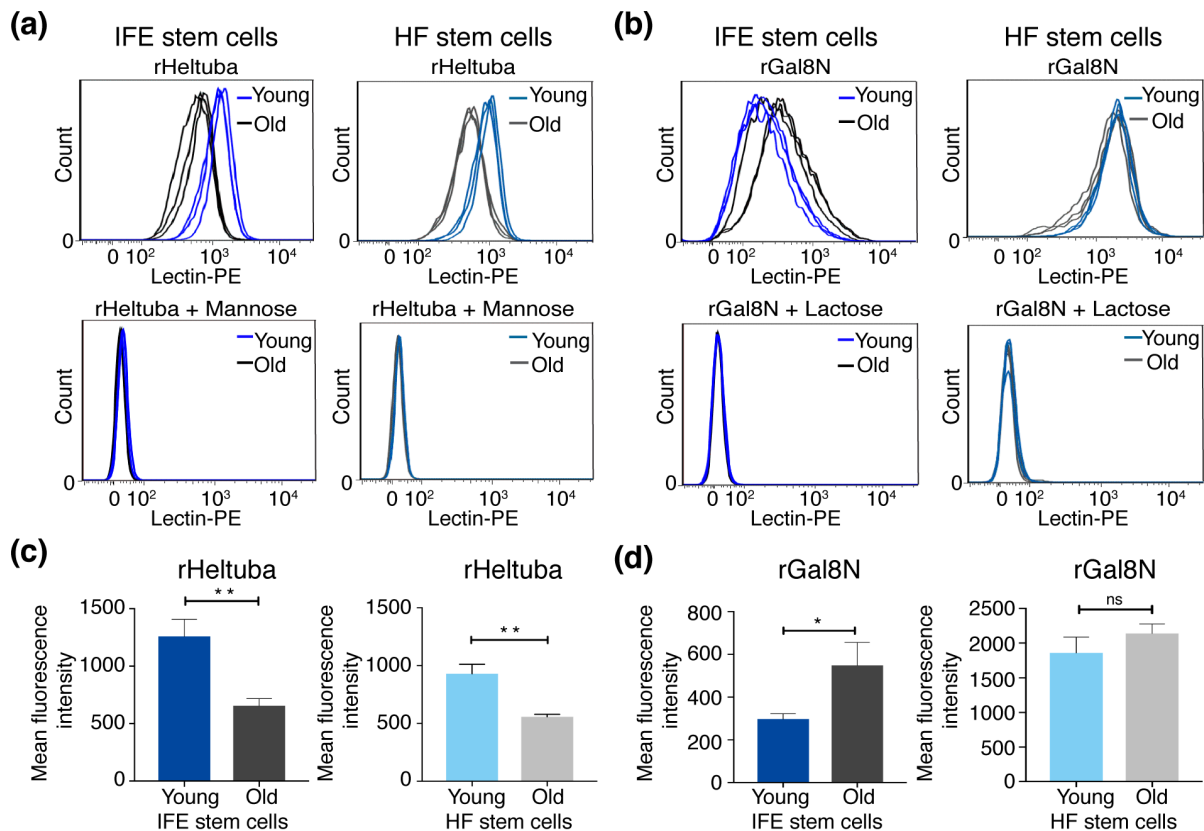


**Figure 5.** The rHeltuba and rGal8N lectins differentially bind to freshly isolated young and old stem cells. (a, b) The histogram shows signal intensities of PE-labeled rHeltuba (1  $\mu\text{g/ml}$ ) (a) or rGal8N (10  $\mu\text{g/ml}$ ) (b) in the interfollicular epidermis (IFE) and hair follicles (HF) detected by flow cytometry.  $N=3$  for young and old mice. Data from each mouse is shown as an individual line. For inhibition of rHeltuba and rGal8N, 0.1M mannose or 0.1M lactose are used, respectively. (c, d) Quantification of mean fluorescence intensity obtained by flow cytometry. Data are shown as means  $\pm$  SD. Statistical analysis is performed using the unpaired Student's t-test. \*\*:  $p < 0.01$ . \*:  $p < 0.05$ . ns: not significant; rGal8N in HF stem cells,  $p = 0.1412$ .

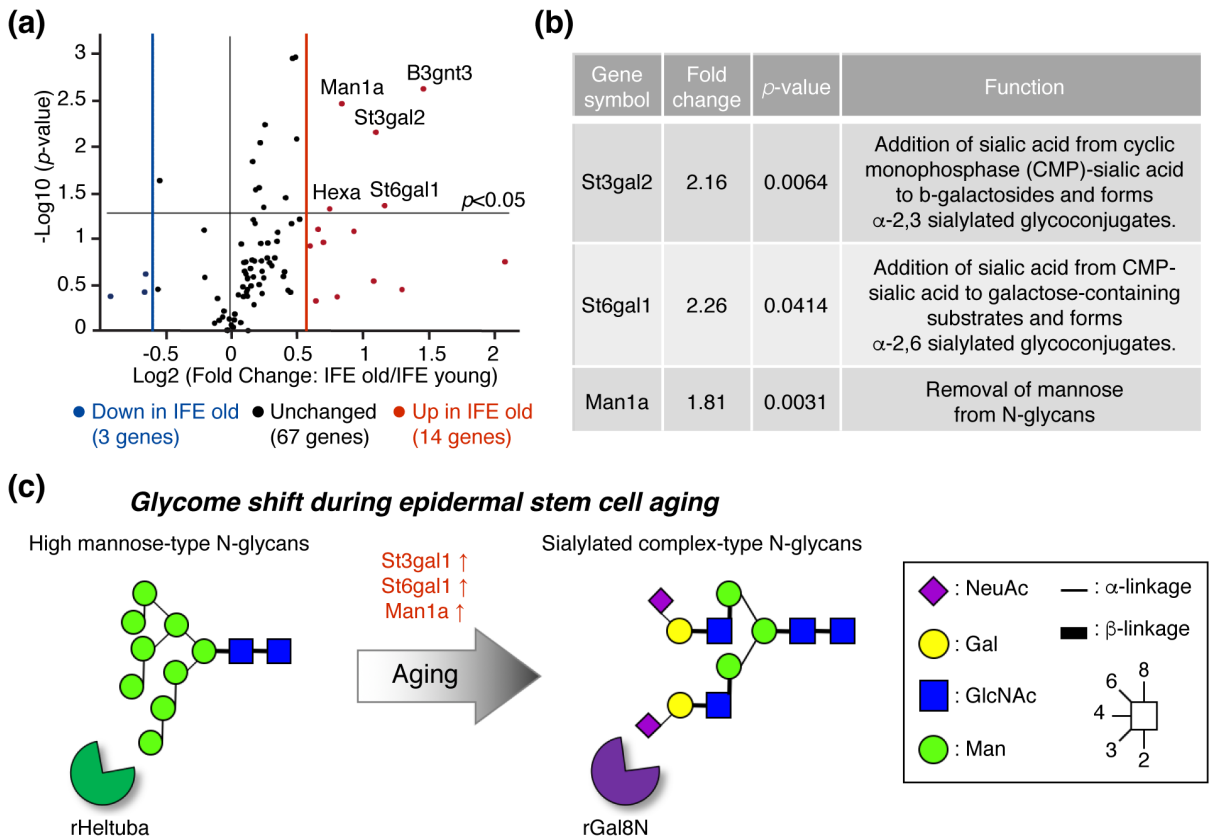


**Figure 6.** Gene expression analysis of glycosylation-related genes using RT2 Profiler PCR array. (a) The volcano plot represents fold change and p-values on x- and y-axis, respectively. The vertical red and blue lines represent a fold change cut-off of  $\geq 1.5$ . (b) Lists of differentially expressed sialyltransferase and mannosidase genes. (c) Schematic representation of the putative

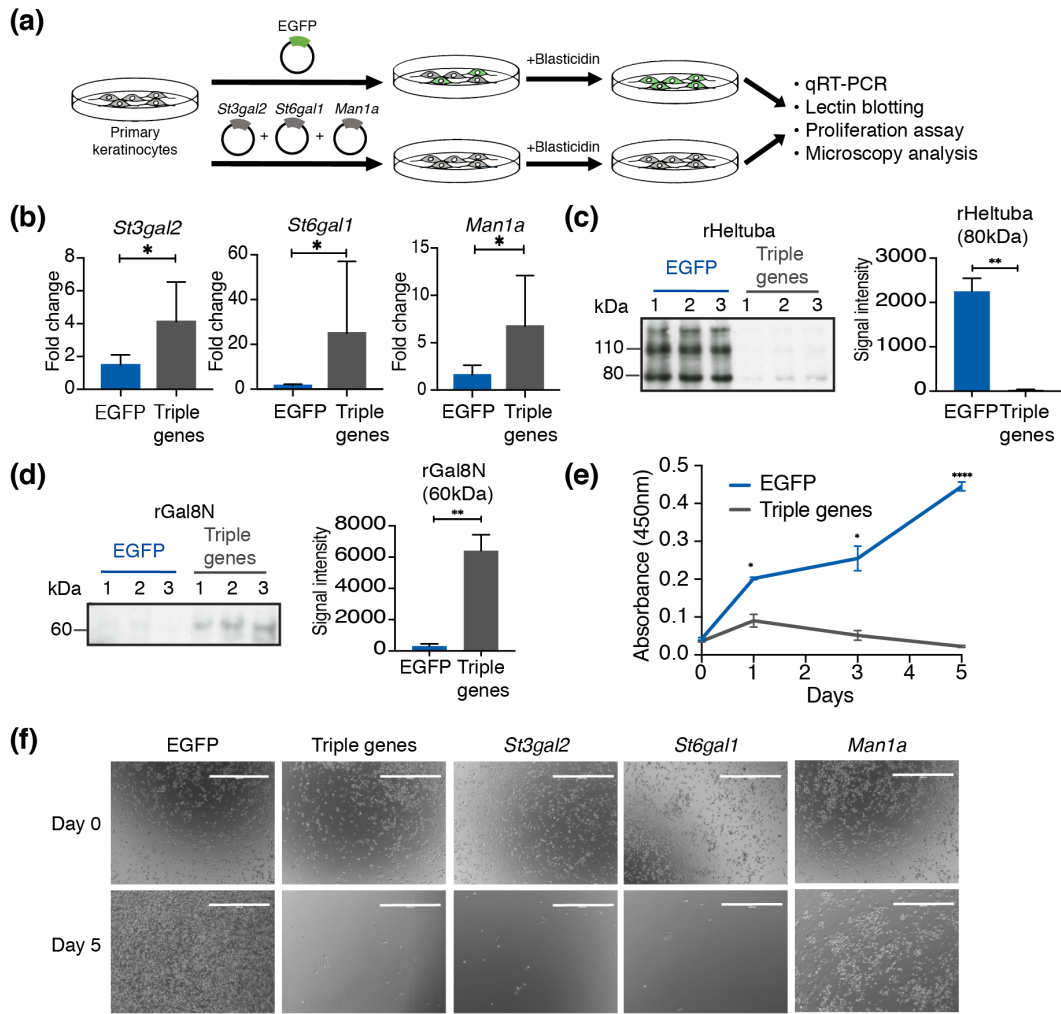


**Figure 7.** Aging-associated glycogene overexpression leads to an impaired keratinocyte growth. (a) Scheme of the glycoprotein overexpression using the lentivirus system. (b) The qRT-PCR of *Man1a*, *St3gal2*, *St6gal1* mRNA expression at 4 days after blasticidin selection ( $N=3$ ). Lenti-EGFP is used as a control. Data are shown as means  $\pm$  SD. Mann-Whitney test. \*\*\*,  $p < 0.001$ . \*\*,  $p < 0.01$ . \*,  $p < 0.05$ . (c, d) Confirmation of glycan changes by lectin blotting using the horseradish peroxidase (HRP)-labeled lectins, rHeltuba (c) and rGal8N (d). One microgram of protein from three independent experiments is applied on each lane. Data are shown as means  $\pm$  SD. Student's *t*-test. \*\*\*,  $p < 0.001$ . \*\*,  $p < 0.01$ . \*,  $p < 0.05$ . The signal intensities of bands with indicated size are quantified. (e) Proliferation assay of primary keratinocytes after overexpressing glycoproteins. The x-axis represents the time points, and the y-axis represents the absorbance at 450 nm. Absorbance is measured at 0, 1, 3, and 5 days post-infection. Data are shown as means  $\pm$  SD. Student's *t*-test. \*\*\*,  $p < 0.001$ . \*\*,  $p < 0.01$ . \*,  $p < 0.05$ . (f) Representative images of the primary keratinocytes infected with lenti-EGFP, or a combination or single lenti-*Man1a*, -*St3gal2*, and -*St6gal1* at day 0 and 5.

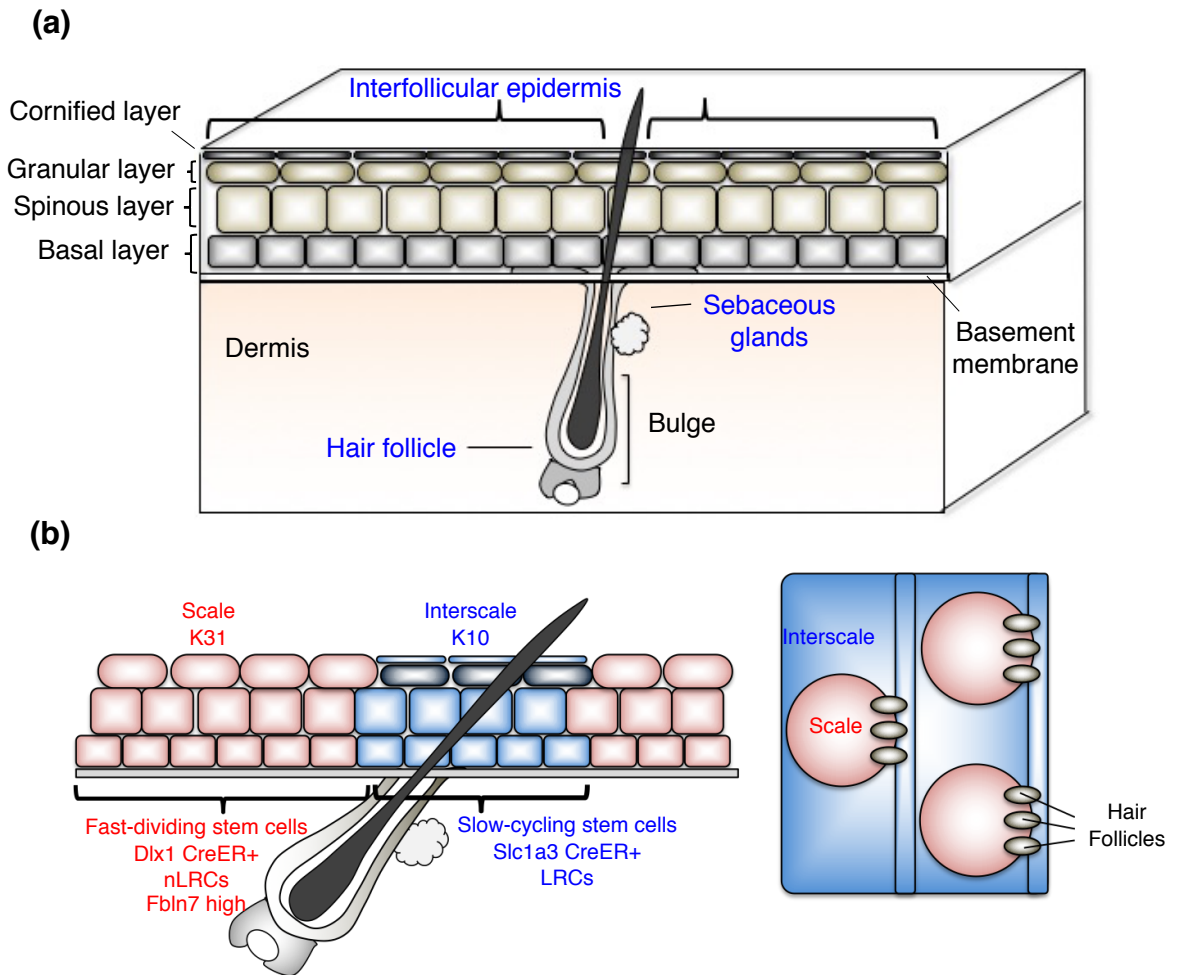


**Figure 8.** Different stem cell populations in the mouse skin. (a) Schematic representation of mouse skin interfollicular epidermis separated by the basement membrane from the dermis, different layers of epidermis are shown along with the bulge and hair-follicle. (b) Diagram showing a sagittal view of mouse scale and interscale in the tail undergoing a different type of keratinization. Region specific markers are shown. The right image shows the whole mount view.

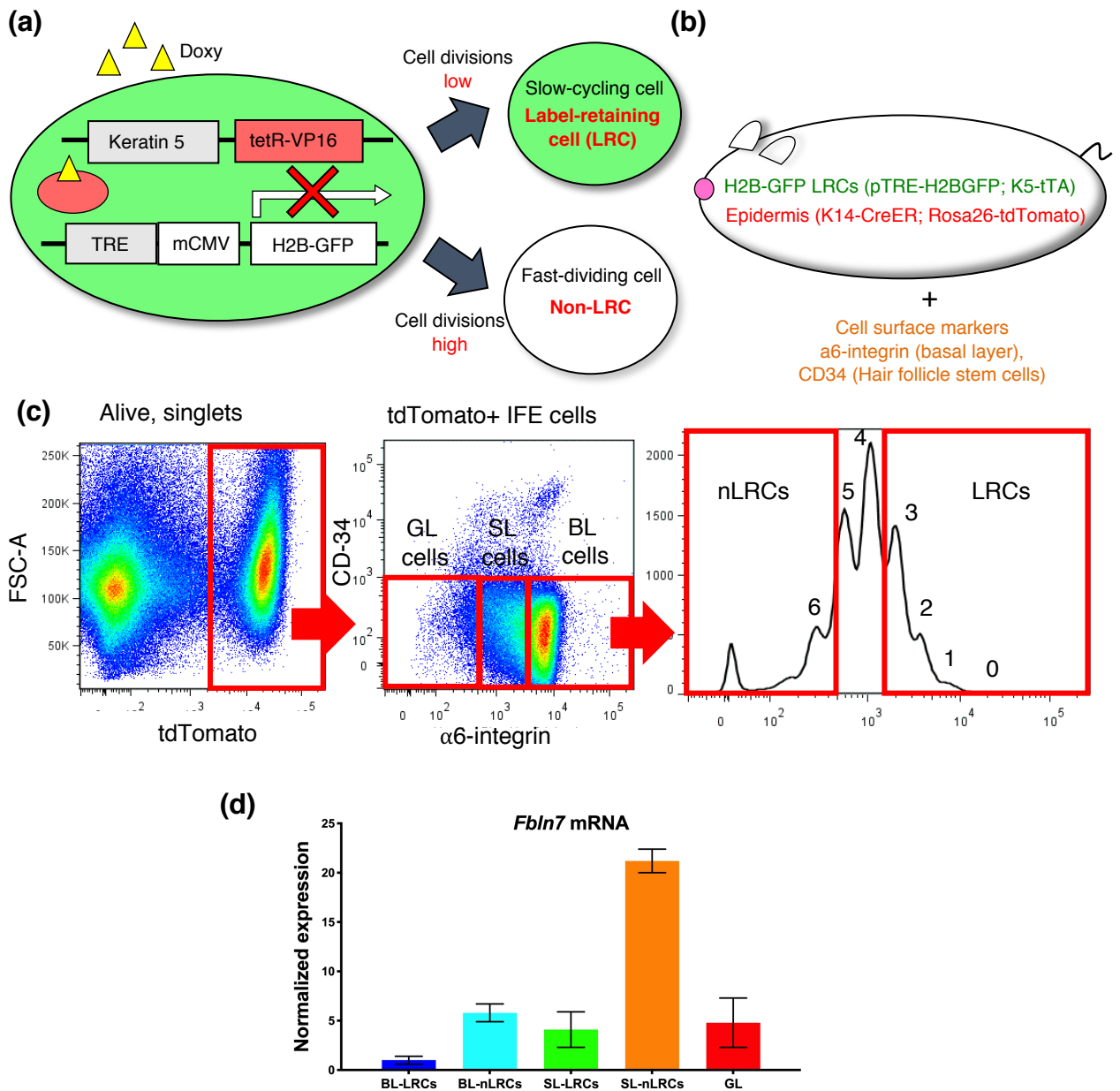


**Figure 9.** H2B-GFP Tet-off system for identifying slow cycling cells. (a) Schematic representation of the H2B-GFP system to detect slow cycling cells as label-retaining cell (LRC)s. (b) Image of quadruple transgenic mouse for isolating basal layer LRCs and non-label retaining cells (nLRCs), spinous layer LRCs and nLRCs, granular layer cells with the markers used. (c) Fluorescence activated cell sorting (FACS) plot for the isolation of LRCs and nLRCs from different layers depicting the number of cell division. (d) Quantitative RT-PCR on FACS-isolated cells. *Fbln7* shows higher expression in basal layer (BL) and spinous layer (SL) non-label retaining cells (nLRCs) as compare to BL and SL label-retaining cells (LRCs) or granular layer (GL).

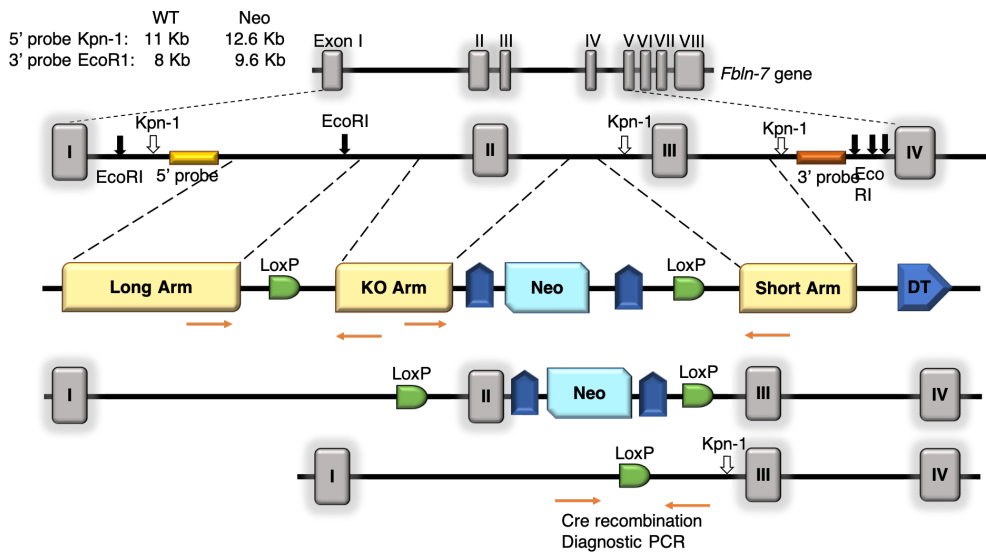
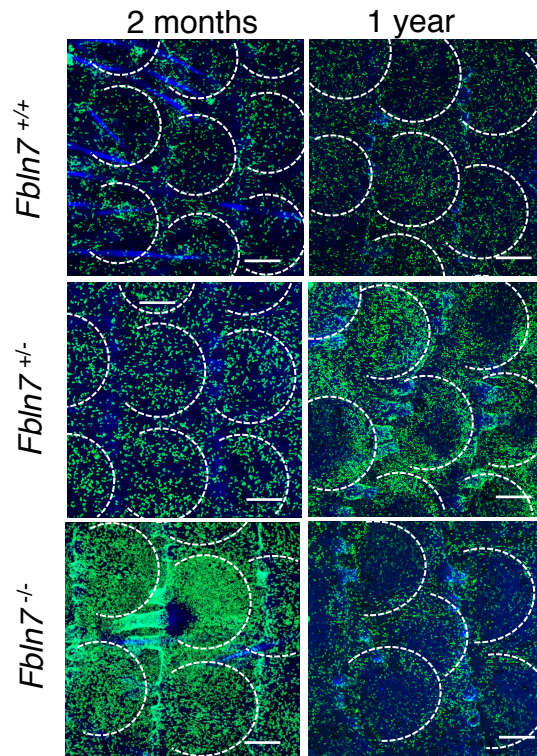
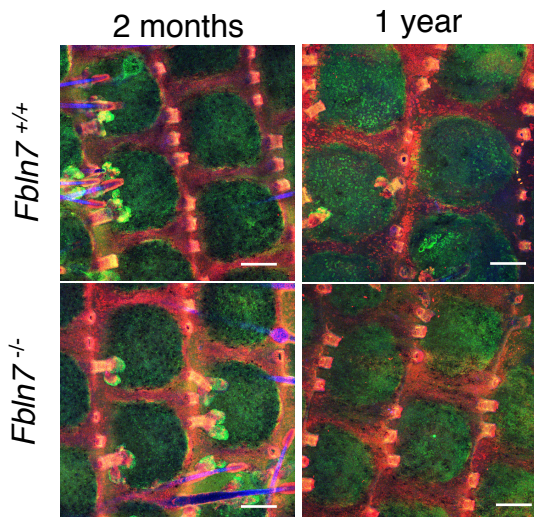


**Figure 10.** *Fbln7* knockout strategy adapted from Tsunazumi et al., 2018.

(a) 2-day BrdU Hoechst



(b) K10 (slow-cycling area)  
K31 (fast-dividing area)



(c) Cleaved Caspase3  
 $\beta$ 4 integrin

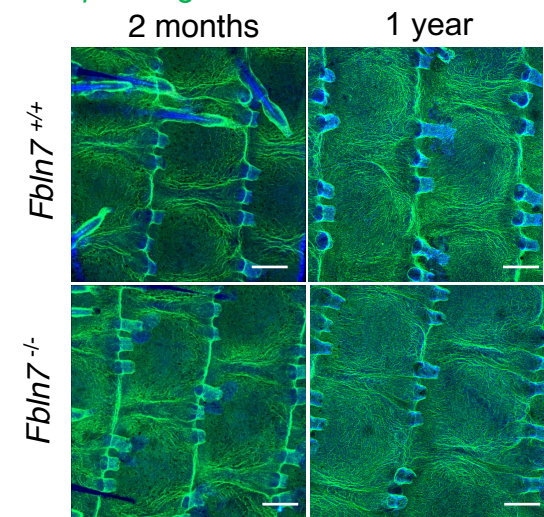


**Figure 11.** Whole-mount staining of tail epidermis in *Fbln7*<sup>-/-</sup> mice. (a) Mice are treated with BrdU for 2 days by drinking water. (b) Whole-mount staining at 2-months and 1 year with differentiation markers, K10 (slow-cycling lineage) and K31 (fast-dividing lineage). (c) Whole-mount staining of cleaved caspase3 to detect apoptotic cells within the basal layer ( $\beta$ 4-integrin<sup>+</sup>). The whole mount image is projected as a Z-stack image from the basal side. Scale bar 200  $\mu$ m (a-c).

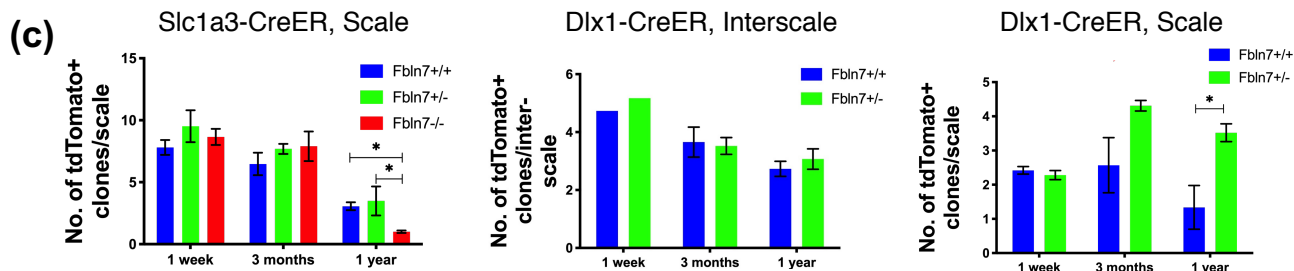
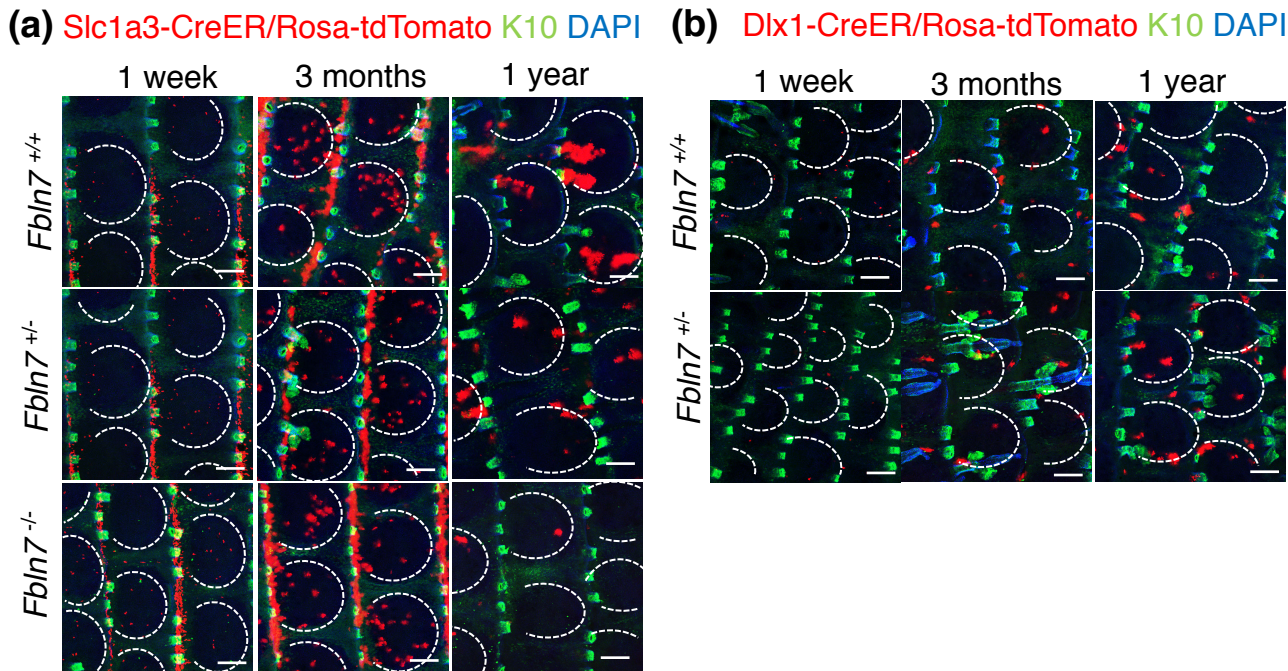


**Figure 12.** Lineage tracing of fast-dividing and slow cycling stem cells. (a) Slc1a3-CreER (a fast-dividing stem cell marker)/Rosa-tdTomato mice are injected with Tamoxifen 25  $\mu\text{g/g}$  body weight for 1 day and chased for 1 week, 3 months and 1 year. (b) Dlx1-CreER (a slow-cycling stem cell marker)/Rosa-tdTomato mice are injected with Tamoxifen 50  $\mu\text{g/g}$  body weight for 1 day and chased for 1 week, 3 months and 1 year. (c) Quantification of the number of clones per area in Slc1a3-CreER (scale region) and Dlx1-CreER (inter-scale and scale regions). The scale area is indicated by white dashed circle.  $N=3$  except Dlx1-CreER at 1 week ( $N=1$ ). Scale bars, 200  $\mu\text{m}$  (a-b).

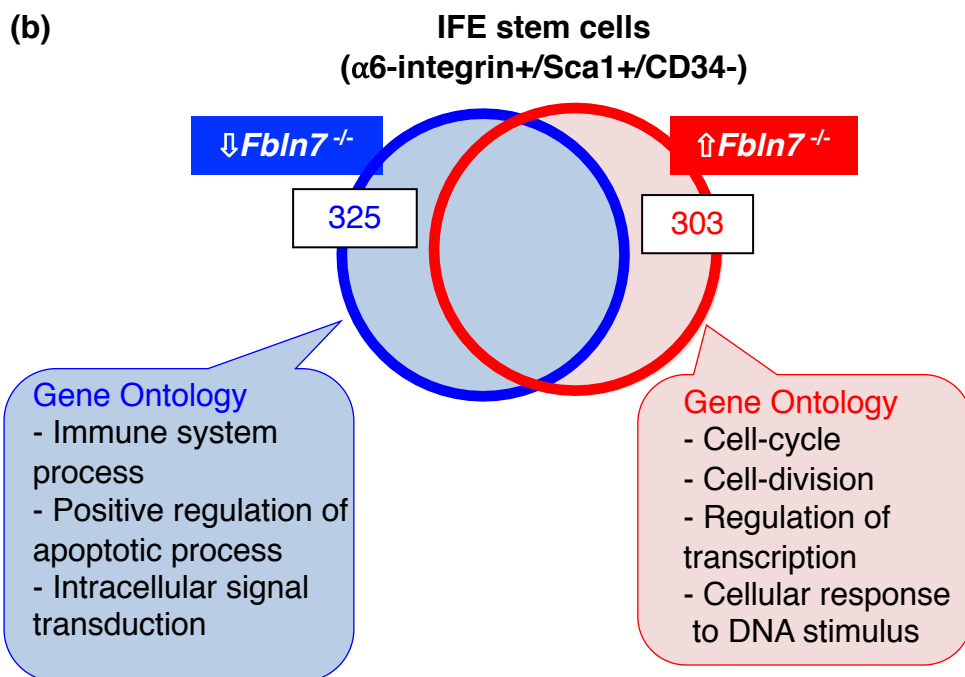
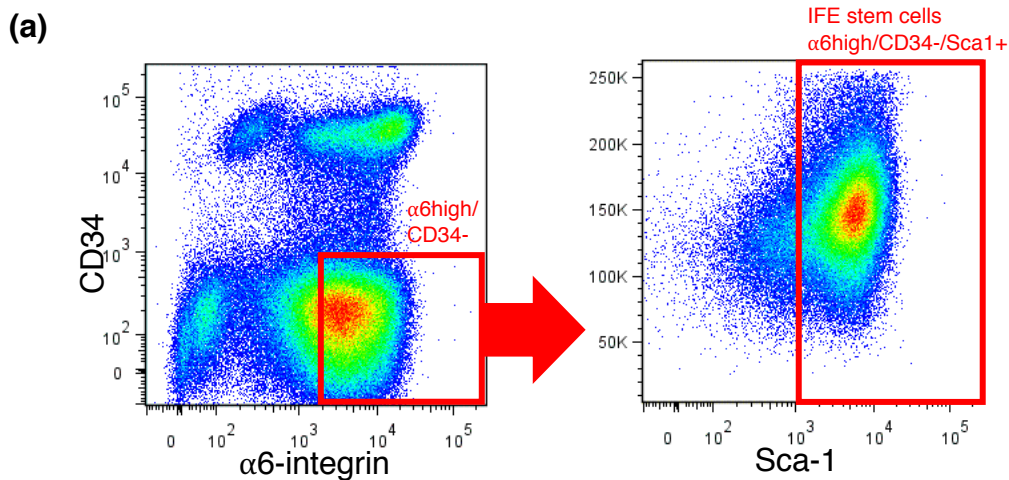


**Figure 13.** RNA-sequencing analysis of *Fbln7*<sup>-/-</sup> epidermal basal cells. (a) Scheme for fluorescence activated cell sorting of mouse interfollicular epidermal (IFE) stem cells from *Fbln7*<sup>-/-</sup> mice for RNA-sequencing analysis. (b) Gene ontology of 628 genes differentially expressed greater than 2-folds in *Fbln7*<sup>-/-</sup> mice



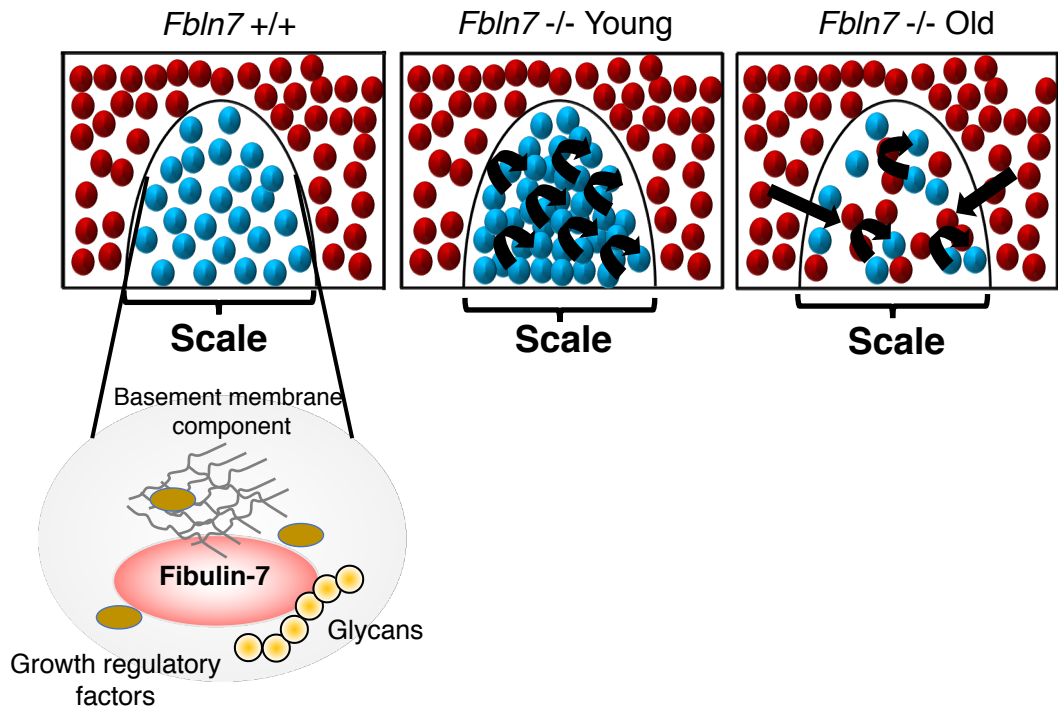


**Figure 15.** Proposed model for the role of Fibulin-7 in maintenance of fast-dividing stem cells (scale region) in the mouse epidermis.